NASA TECHNICAL NOTE

NASA TN D-2815

NASA TN D-2815

EFFECT OF EDGE LOADINGS ON THE VIBRATION OF RECTANGULAR PLATES WITH VARIOUS BOUNDARY CONDITIONS

by George E. Weeks and John L. Shideler

Langley Research Center
Langley Station, Hampton, Va.

NATIONAL AERONAUTICS AND SPACE ADMINISTRATION • WASHINGTON, D. C. • MAY 1965

ERRATA

NASA Technical Note D-2815

EFFECT OF EDGE LOADINGS ON THE
VIBRATION OF RECTANGULAR PLATES WITH
VARIOUS BOUNDARY CONDITIONS

By George E. Weeks and John L. Shideler
May 1965

Page 14, figure 6: The two curves labeled $n = 2$ and $n = 4$ should be replaced with the two curves shown on the attached figure.

Page 23: The second of equations (B1) has an error in sign in the denominator. The minus sign before $\frac{4}{q_y}$ should be a plus sign, so that the corrected form of the equation reads

$$\left(\frac{C_1}{C_0}\right)_A = 4\delta^2\left[\frac{-1 + \sin^2\delta\left(\frac{4}{q_y} + 1 + \frac{2}{\delta \tanh \delta} - \frac{1}{\tanh^2\delta}\right)}{1 + \sin^2\delta\left(\frac{4}{q_y} + 1 - \frac{1}{\tanh^2\delta}\right)}\right] \qquad \text{(Asymmetrical)}$$

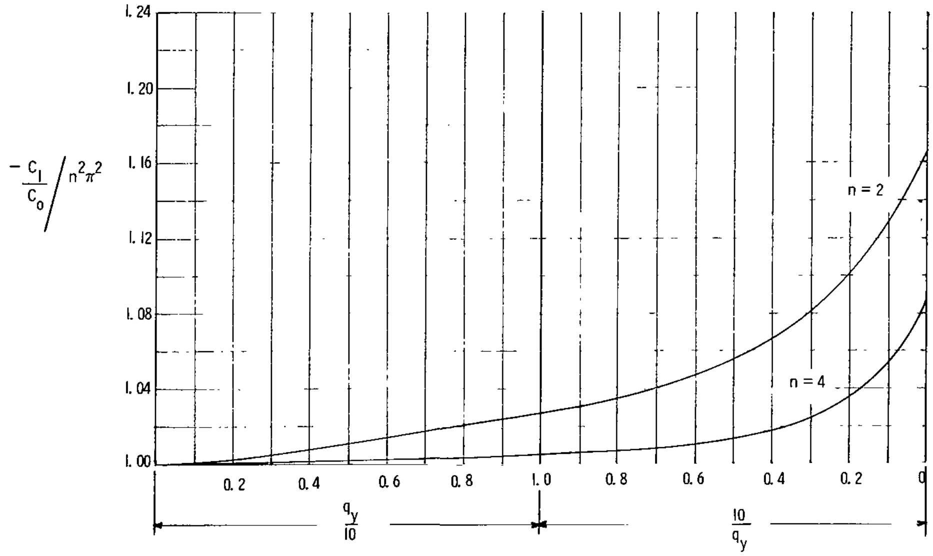

Corrections for Figure 6. - Variation of C_1/C_0 with rotational restraint coefficient q_y for first two asymmetrical modes.

NASA-Langley, 1967

Issued 6-7-67

NASA TN D-2815

EFFECT OF EDGE LOADINGS ON THE VIBRATION OF RECTANGULAR PLATES WITH VARIOUS BOUNDARY CONDITIONS

By George E. Weeks and John L. Shideler

Langley Research Center
Langley Station, Hampton, Va.

NATIONAL AERONAUTICS AND SPACE ADMINISTRATION

For sale by the Clearinghouse for Federal Scientific and Technical Information
Springfield, Virginia 22151 – Price $2.00

EFFECT OF EDGE LOADINGS ON THE VIBRATION OF RECTANGULAR PLATES WITH VARIOUS BOUNDARY CONDITIONS

By George E. Weeks and John L. Shideler
Langley Research Center

SUMMARY

The natural vibration characteristics of flat orthotropic rectangular plates with inplane loads and various boundary conditions are investigated theoretically. A set of frequency equations is derived which is valid for plates having edges simply supported, clamped, or elastically restrained against rotation. The solutions to these frequency equations are presented in terms of two general parameters which are functions of length-width ratio, stiffness ratios, frequency, and inplane stress. These solutions are exact if one pair of opposite edges is simply supported, otherwise the solutions are approximate. However, these approximate solutions are shown to be in excellent agreement with converged modal solutions. The results of the analysis are tabulated so that, for the boundary conditions considered, the buckling stress, and the variation of frequency and modal behavior with inplane stress can be quickly and accurately determined for large ranges of length-width ratio, stiffness ratio, and inplane stress.

INTRODUCTION

External surfaces of flight vehicles have been shown to be susceptible to various types of aeroelastic instabilities - the most noticeable of which is flutter. However, flutter analyses are, to a large extent, dependent on predictions of vibration and buckling characteristics of surface structural components, particularly under inplane loading conditions. One of the most basic of these structural components is the rectangular plate.

The problem of determining the natural vibration characteristics of isotropic rectangular plates in the absence of normal and inplane loading with various boundary conditions has been the object of numerous theoretical and experimental investigations. (See, for example, refs. 1 to 5.) In fewer instances, the effect of inplane loading on simply supported or clamped plates has been studied. (See refs. 5 to 10.) However, the more general cases of isotropic and orthotropic plates with elastically restrained edges subjected to inplane loads have received much less attention.

The most comprehensive treatment of the effect of inplane loading on the vibration of plates with elastically restrained edges is due to Schulman (ref. 11) who treats the case of an isotropic rectangular plate subjected to inplane loading with elastic restraints along the longitudinal edges and with simple supports on the lateral edges. The constant inplane loads throughout the plate were assumed to be due to restraint against thermal expansion. The exact frequency equation was derived but was solved exactly for only one given length-width ratio and elastic restraint coefficient. However, two approximate solutions to the vibration problem were presented which were based on: (1) the assumption that the mode shapes remain unaltered with increasing temperature, thus obtaining a linear relationship between the frequency parameter and inplane loading and (2) an energy approach using Lagrange's equations. Results for both methods were presented in terms of a frequency-temperature relationship (ref. 11).

In the analysis that follows, an orthotropic plate with biaxial inplane loading and rotational springs of equal elastic restraint on opposite edges is considered. The magnitude of elastic rotational restraint is defined by a restraint coefficient having a value of zero for simple supports and infinity for clamped supports. Starting with the governing partial differential equation, the frequency equations are derived. These equations are exact if one pair of edges is simply supported but approximate if supported otherwise. The frequency equations are then solved for several representative values of the rotational restraint coefficient, including the special cases corresponding to simple and clamped supports.

The results are presented in tabular and graphical forms in terms of two general parameters which are functions of frequency, length-width ratio, stiffness ratios, and inplane stress. With these results, the frequency-stress relationship and buckling characteristics of a plate can be quickly and accurately determined for large ranges of length-width ratio, stiffness ratio, inplane loading, and rotational restraint at the boundaries.

SYMBOLS

$\bar{A},\bar{B}$ parameters defined by equation (4)

a,b plate length in x-direction and y-direction, respectively

B_1,B_2,B_3,B_4 constants of integration appearing in equation (10)

B_1',B_2',B_3',B_4' constants of integration appearing in equation (14)

C_0,C_1,C_2 coefficients defined by equation (7)

$D = \dfrac{Eh^3}{12\left(1 - \mu^2\right)}$ bending stiffness of an isotropic plate

D_x, D_y	plate bending stiffness in x- and y-directions, respectively
D_{xy}	plate twisting stiffness
D_1, D_{12}, D_2	plate stiffness coefficients defined by equation (6)
E	Young's modulus
e	base of Naperian logarithm
h	plate thickness
$i = \sqrt{-1}$	
k_x	nondimensional stress coefficient, $\frac{N_x b^2}{\pi^2 D_1}$
k_y	nondimensional stress coefficient, $\frac{N_y b^2}{\pi^2 D_1}$
m, n	integers defining mode number in x- and y-direction, respectively
N_x	inplane loading in x-direction, positive in compression
N_y	inplane loading in y-direction, positive in compression
$q_x = \frac{a\theta_x}{D_1}$	rotational restraint coefficient on boundary, $x = \pm\frac{a}{2}$
$q_y = \frac{b\theta_y}{D_2}$	rotational restraint coefficient on boundary, $y = \pm\frac{b}{2}$
t	time
w	vertical deflection of plate
X, Y	assumed variables separable solution of differential equation (1a)
x, y	Cartesian coordinates (See fig. 1.)
$\alpha, \beta, \overline{\beta}$	nondimensional parameters defined by equations (11) and (13)
ξ, η	nondimensional coordinates in x- and y-direction, respectively, $\xi = \frac{x}{a}$, $\eta = \frac{y}{b}$
δ	nondimensional parameter used when $\alpha = \beta$

θ_x, θ_y spring constant of rotational springs supporting plate on the boundaries $x = \pm\frac{a}{2}$ and $y = \pm\frac{b}{2}$, respectively

μ Poisson's ratio for isotropic plate

μ_x, μ_y Poisson's ratio in x- and y-direction, respectively

ρ mass density per unit area

ω natural frequency

ω_o nondimensional frequency parameter, $\sqrt{\frac{\pi^4 D_1}{a^4 \rho}}$

Subscripts:

S symmetrical mode

A asymmetrical mode

ANALYSIS

Solution to Plate Equation

The plate configuration and coordinate system used are shown in figure 1. The plate is subjected to inplane forces N_x and N_y, defined positive in compression. The boundary conditions are such that uniform rotational restraint on opposite edges is provided by a restoring moment per unit length which is proportional to the edge angle of rotation. Also, support conditions are such that the transverse deflection on all edges is zero.

With inplane loads, the differential equation of small deflection theory governing vibrations of a flat orthotropic plate is (ref. 12)

$$\frac{D_x}{1 - \mu_x\mu_y}\frac{\partial^4 w}{\partial x^4} + 2\left(D_{xy} + \frac{\mu_y D_x}{1 - \mu_x\mu_y}\right)\frac{\partial^4 w}{\partial x^2 \partial y^2} + \frac{D_y}{1 - \mu_x\mu_y}\frac{\partial^4 w}{\partial y^4} + N_x\frac{\partial^2 w}{\partial x^2}$$

$$+ N_y\frac{\partial^2 w}{\partial y^2} + \rho\frac{\partial^2 w}{\partial t^2} = 0 \qquad (1a)$$

with boundary conditions -

$$\left.\begin{aligned}
&\frac{D_x}{1 - \mu_x\mu_y}\frac{\partial^2 w}{\partial x^2} - \theta_x \frac{\partial w}{\partial x} = 0 \quad \text{and} \quad w = 0 \qquad \text{at} \quad x = -\frac{a}{2} \\
&\frac{D_x}{1 - \mu_x\mu_y}\frac{\partial^2 w}{\partial x^2} + \theta_x \frac{\partial w}{\partial x} = 0 \quad \text{and} \quad w = 0 \qquad \text{at} \quad x = +\frac{a}{2}
\end{aligned}\right\} \tag{1b}$$

$$\left.\begin{aligned}
&\frac{D_y}{1 - \mu_x\mu_y}\frac{\partial^2 w}{\partial y^2} - \theta_y \frac{\partial w}{\partial y} = 0 \quad \text{and} \quad w = 0 \qquad \text{at} \quad y = -\frac{b}{2} \\
&\frac{D_y}{1 - \mu_x\mu_y}\frac{\partial^2 w}{\partial y^2} + \theta_y \frac{\partial w}{\partial y} = 0 \quad \text{and} \quad w = 0 \qquad \text{at} \quad y = +\frac{b}{2}
\end{aligned}\right\} \tag{1c}$$

where θ_x and θ_y are the spring constants of the rotational springs on the boundaries $x = \pm\frac{a}{2}$ and $y = \pm\frac{b}{2}$, respectively; D_x and D_y are the plate bending stiffnesses in the x- and y-directions, respectively; and D_{xy} is the plate twisting stiffness. An exact closed-form solution to equation (1a) is known only for the special case where two opposite edges are simply supported. However, an approximate solution can be obtained for the general case in the following manner. Assume

$$w(x,y,t) = X\left(\frac{x}{a}\right)Y\left(\frac{y}{b}\right)e^{i\omega t} \tag{2}$$

where ω is the natural frequency; $Y\left(\frac{y}{b}\right)$ is some assumed mode shape that satisfies the boundary conditions on the boundaries $y = \pm\frac{b}{2}$; and $X\left(\frac{x}{a}\right)$ is a mode shape to be determined. Substitution of equation (2) into equation (1a), multiplication by $Y\left(\frac{y}{b}\right)$, and integration over the width with respect to y yields an ordinary differential equation in $X\left(\frac{x}{a}\right)$. This procedure is essentially the first step of

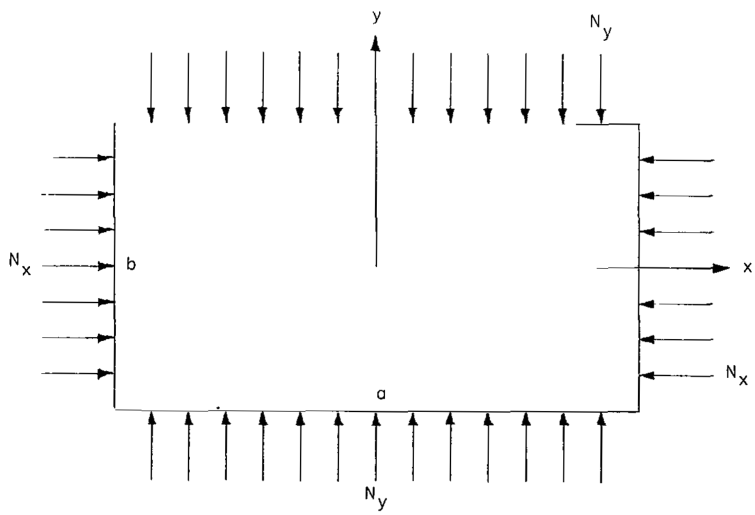

Figure 1.- Geometry and coordinate system.

a Galerkin procedure which, for this case, is equivalent to the method of Kantorovich. (See ref. 13.) After nondimensionalization, this procedure yields

$$X^{IV}(\xi) - 2\pi^2\bar{A}X''(\xi) - \pi^4\bar{B}X(\xi) = 0 \tag{3}$$

where

$$\left.\begin{aligned} \bar{A} &= -\left(\frac{a}{b}\right)^2\left[\left(\frac{D_{12}}{D_1}\right)\left(\frac{1}{\pi^2}\right)\left(\frac{C_1}{C_0}\right) + \frac{k_x}{2}\right] \\ \bar{B} &= \left(\frac{\omega}{\omega_0}\right)^2 - \left(\frac{a}{b}\right)^4\left[\left(\frac{D_2}{D_1}\right)\left(\frac{1}{\pi^4}\right)\left(\frac{C_2}{C_0}\right) + \frac{k_y}{\pi^2}\frac{C_1}{C_0}\right] \end{aligned}\right\} \tag{4}$$

$$k_x = \frac{N_x b^2}{\pi^2 D_1} \qquad k_y = \frac{N_y b^2}{\pi^2 D_1} \qquad {\omega_0}^2 = \frac{\pi^4 D_1}{a^4 \rho} \tag{5}$$

$$D_1 = \frac{D_x}{1 - \mu_x\mu_y} \qquad D_{12} = D_{xy} + \frac{\mu_y D_x}{1 - \mu_x\mu_y} \qquad D_2 = \frac{D_y}{1 - \mu_x\mu_y} \tag{6}$$

$$C_0 = \int_{-1/2}^{1/2} Y^2(\eta)d\eta \qquad C_1 = \int_{-1/2}^{1/2} Y(\eta)Y''(\eta)d\eta \qquad C_2 = \int_{-1/2}^{1/2} Y(\eta)Y^{IV}(\eta)d\eta \tag{7}$$

and

$$\xi = \frac{x}{a} \qquad \eta = \frac{y}{b} \tag{8}$$

The primes and Roman numeral superscripts denote differentiation with respect to ξ and η. Note that the parameters $\bar{A}$ and $\bar{B}$ depend on the assumed shape $Y(\eta)$ through the coefficients C_1/C_0 and C_2/C_0. Thus equation (3) is an approximation unless $Y(\eta)$ is the exact mode shape in the y-direction.

The boundary conditions (eqs. (1b)) become -

$$\left.\begin{aligned} X''(\xi) - q_x X'(\xi) &= 0 \quad \text{and} \quad X(\xi) = 0 \qquad \text{at} \quad \xi = -1/2 \\ X''(\xi) + q_x X'(\xi) &= 0 \quad \text{and} \quad X(\xi) = 0 \qquad \text{at} \quad \xi = 1/2 \end{aligned}\right\} \tag{9}$$

where

$$q_x = \frac{a\theta_x}{D_1}$$

The exact solution to equation (3) for unequal roots of the characteristic equation is $X(\xi) = X_A + X_S$, where

$$\left.\begin{aligned} X_S &= B_1 \cos 2\alpha\xi + B_2 \cosh 2\beta\xi \\ X_A &= B_3 \sin 2\alpha\xi + B_4 \sinh 2\beta\xi \end{aligned}\right\} \tag{10}$$

and

$$\alpha = \frac{\pi}{2}\left(-\bar{A} + \sqrt{\bar{A}^2 + \bar{B}}\right)^{1/2} \qquad \beta = \frac{\pi}{2}\left(\bar{A} + \sqrt{\bar{A}^2 + \bar{B}}\right)^{1/2} \tag{11}$$

Note that both α and β are functions of frequency since they are functions of $\bar{B}$. Equations (11) can be solved for $\bar{A}$ and $\bar{B}$ in terms of α and β to get

$$\bar{A} = \frac{2}{\pi^2}\left(\beta^2 - \alpha^2\right) \qquad \bar{B} = \frac{16}{\pi^4}\alpha^2\beta^2 \tag{12}$$

The parameters $\bar{A}$ and $\bar{B}$ can be either positive or negative. For $\bar{B}$ positive, both α and β are always real. For $\bar{B}$ negative, α and β would be complex when $\left|\bar{B}\right| > \bar{A}^2$. This could occur for certain loading conditions and negative rotational restraint. But for this investigation only positive values of rotational restraint are considered so that β is pure imaginary and α real when $\bar{B}$ is negative. Thus, for convenience, define

$$\bar{\beta} = i\beta = \frac{\pi}{2}\left(-\bar{A} - \sqrt{\bar{A}^2 + \bar{B}}\right)^{1/2} \tag{13}$$

such that for $\bar{B}$ negative, the solution to equation (3) is

$$\left.\begin{aligned} X_S &= B_1' \cos 2\alpha\xi + B_2' \cos 2\bar{\beta}\xi \\ X_A &= B_3' \sin 2\alpha\xi + B_4' \sin 2\bar{\beta}\xi \end{aligned}\right\} \tag{14}$$

with

$$\bar{A} = -\frac{2}{\pi^2}\left(\beta^2 + \alpha^2\right) \qquad \bar{B} = -\frac{16}{\pi^4}\alpha^2\bar{\beta}^2 \tag{15}$$

Frequency Equations and Deflection Functions

Application of the boundary conditions (eqs. (9)) to equations (10) and equations (14) results in two sets of four linear homogeneous equations in B_1, B_2, B_3, B_4, and B_1', B_2', B_3', B_4'; one set is for $\bar{B}$ positive and one set

for $\bar{B}$, negative. These equations have nontrivial solutions if, and only if, the determinants of the coefficients vanish. Further, the expansion of each of these determinants can be reduced by factoring into equations for symmetrical and asymmetrical modes. The resulting frequency equations for $\bar{B}$ positive are -

$$\left.\begin{aligned} &2\left(\alpha^2 + \beta^2\right) + q_x(\alpha \tan \alpha + \beta \tanh \beta) = 0 \qquad &\text{(Symmetrical)} \\ &2\left(\alpha^2 + \beta^2\right) - q_x(\alpha \cot \alpha - \beta \coth \beta) = 0 \qquad &\text{(Asymmetrical)} \end{aligned}\right\} \tag{16}$$

and for $\bar{B}$ negative are -

$$\left.\begin{aligned} &2\left(\alpha^2 - \bar{\beta}^2\right) + q_x(\alpha \tan \alpha - \bar{\beta} \tan \bar{\beta}) = 0 \qquad &\text{(Symmetrical)} \\ &2\left(\alpha^2 - \bar{\beta}^2\right) - q_x(\alpha \cot \alpha - \bar{\beta} \cot \bar{\beta}) = 0 \qquad &\text{(Asymmetrical)} \end{aligned}\right\} \tag{17}$$

The corresponding deflection functions for positive $\bar{B}$ are -

$$\left.\begin{aligned} &X_S = \cos 2\alpha\xi - \frac{\cos \alpha}{\cosh \beta} \cosh 2\beta\xi \qquad &\text{(Symmetrical)} \\ &X_A = \sin 2\alpha\xi - \frac{\sin \alpha}{\sinh \beta} \sinh 2\beta\xi \qquad &\text{(Asymmetrical)} \end{aligned}\right\} \tag{18}$$

and for negative $\bar{B}$ are -

$$\left.\begin{aligned} &X_S = \cos 2\alpha\xi - \frac{\cos \alpha}{\cos \bar{\beta}} \cos 2\bar{\beta}\xi \qquad &\text{(Symmetrical)} \\ &X_A = \sin 2\alpha\xi - \frac{\sin \alpha}{\sin \bar{\beta}} \sin 2\bar{\beta}\xi \qquad &\text{(Asymmetrical)} \end{aligned}\right\} \tag{19}$$

For the special case of simple supports, it can be shown that $\alpha = \frac{m\pi}{2}$ and that equations (18) and (19) reduce to the well-known equations

$$\left.\begin{aligned} &X_S(\xi) = \cos m\pi\xi \qquad &(m = 1, 3, 5, \ldots) \\ &X_A(\xi) = \sin m\pi\xi \qquad &(m = 2, 4, 6, \ldots) \end{aligned}\right\} \tag{20}$$

Substitution of equations (20) into equation (3) yields the following relation between $\bar{A}$ and $\bar{B}$

$$m^4 + 2\bar{A}m^2 - \bar{B} = 0 \tag{21}$$

RESULTS AND DISCUSSION

The frequency equations (16) and (17) were solved for α and β or $\bar{\beta}$ in such a manner as to give the six lowest frequencies for a given value of q_x. The parameters $\bar{A}$ and $\bar{B}$ were calculated from either equation (12) or equation (15). The results are tabulated in tables 1 to 4 for $q_x = \infty$, 40, 10, and 2, respectively. Results are also presented in figures 2, 3, and 4 to show the variation of $\bar{B}$ with $\bar{A}$ for $q_x = 0$, ∞, and 10, respectively.

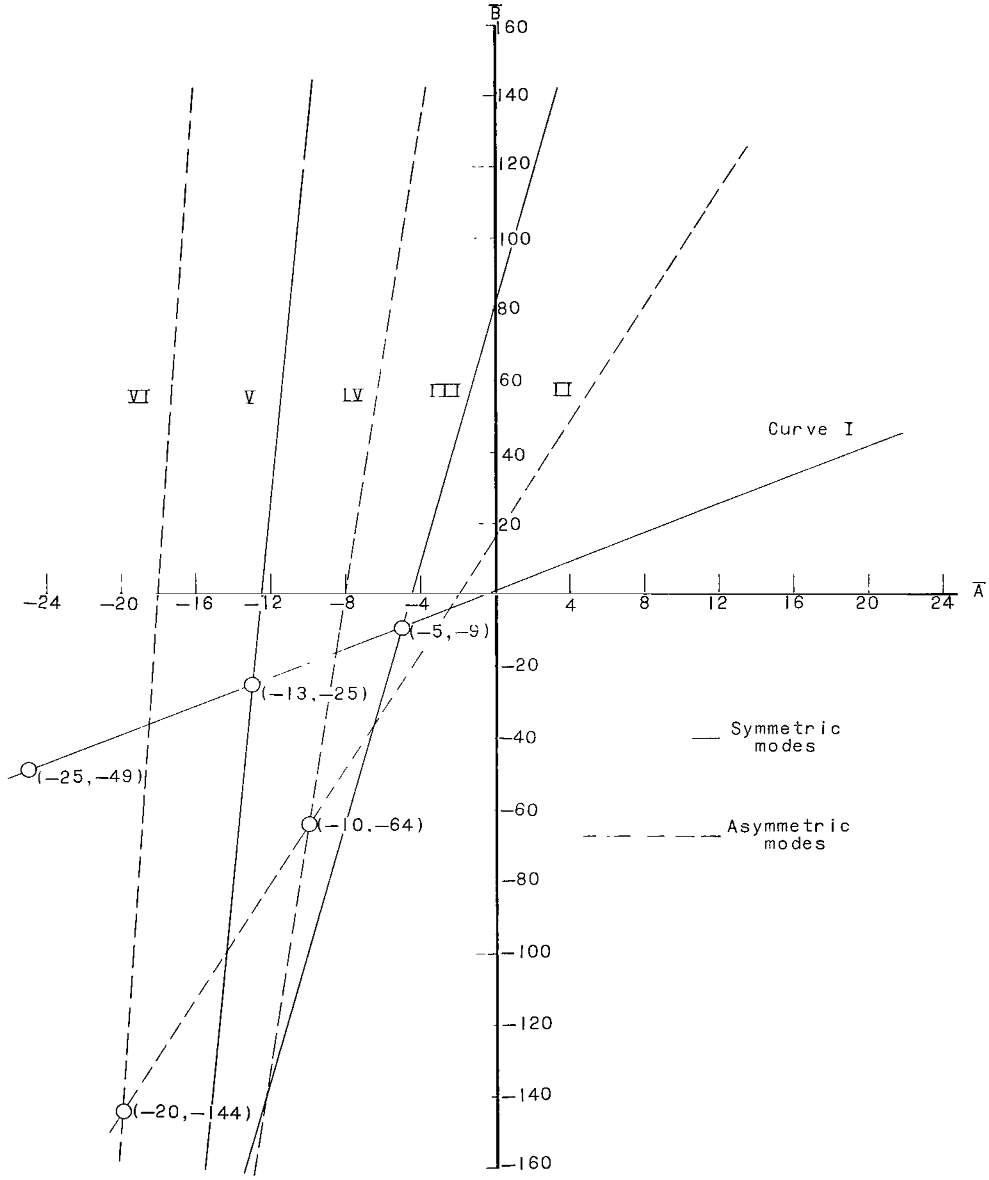

Figure 2.- Variation of $\bar{B}$ with $\bar{A}$ for a plate simply supported on boundaries $x = \pm\frac{a}{2}$. $q_x = 0$.

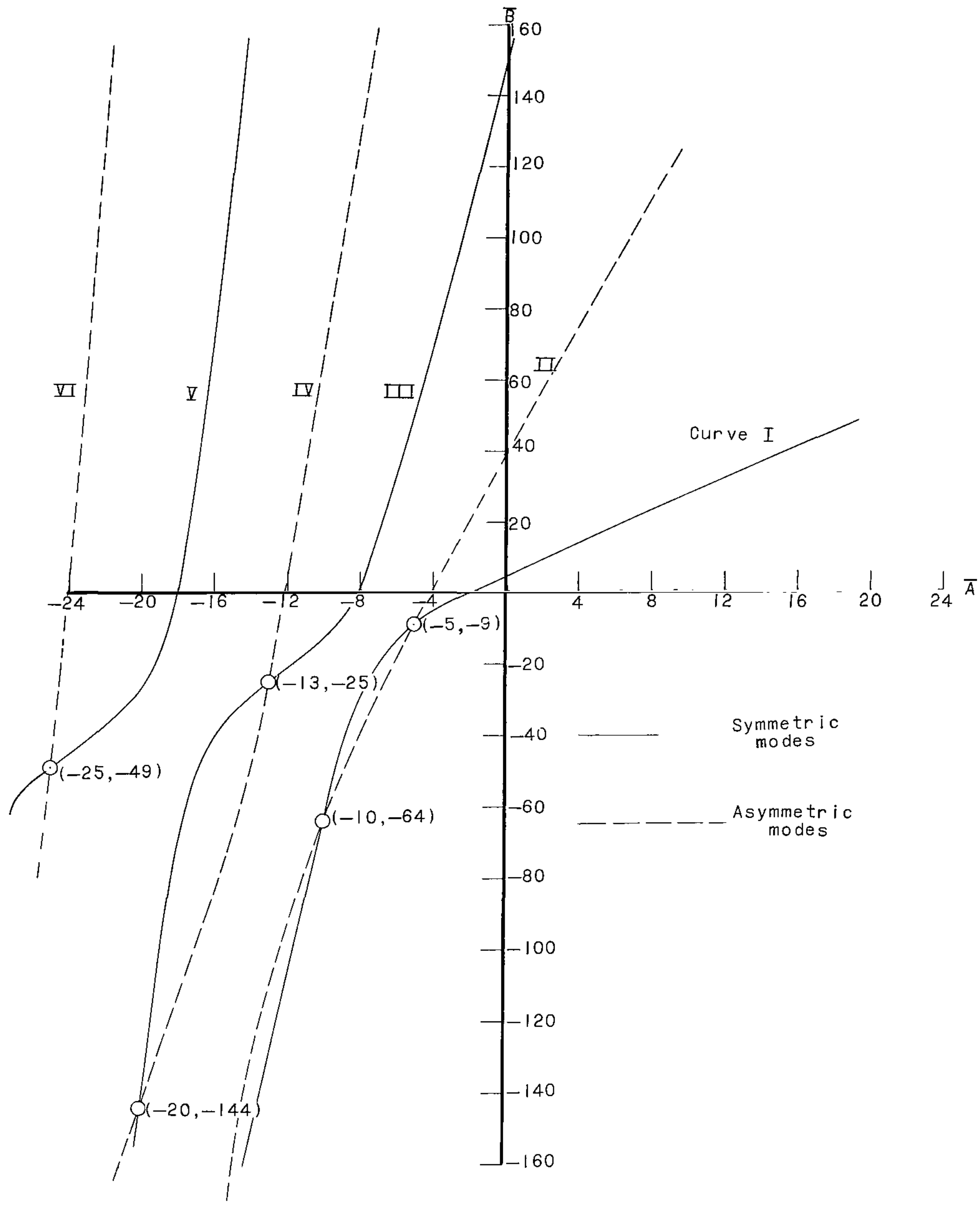

Figure 3.- Variation of $\bar{B}$ with $\bar{A}$ for plate clamped on boundaries $x = \pm\frac{a}{2}$. $q_x = \infty$.

The headings "curve I, II," and so on, in the tables refer to the similarly labeled curves on figures 2 to 4. The mode shapes are defined in the tables and throughout this report by a mode number m in the x-direction, (n in the y-direction) indicating $m - 1$ $(n - 1)$ lines of zero deflection. However, it should be noted that, with this definition, no restriction has been placed on the number of lines of inflection that may occur in any given mode. The reason for this important distinction will become apparent later.

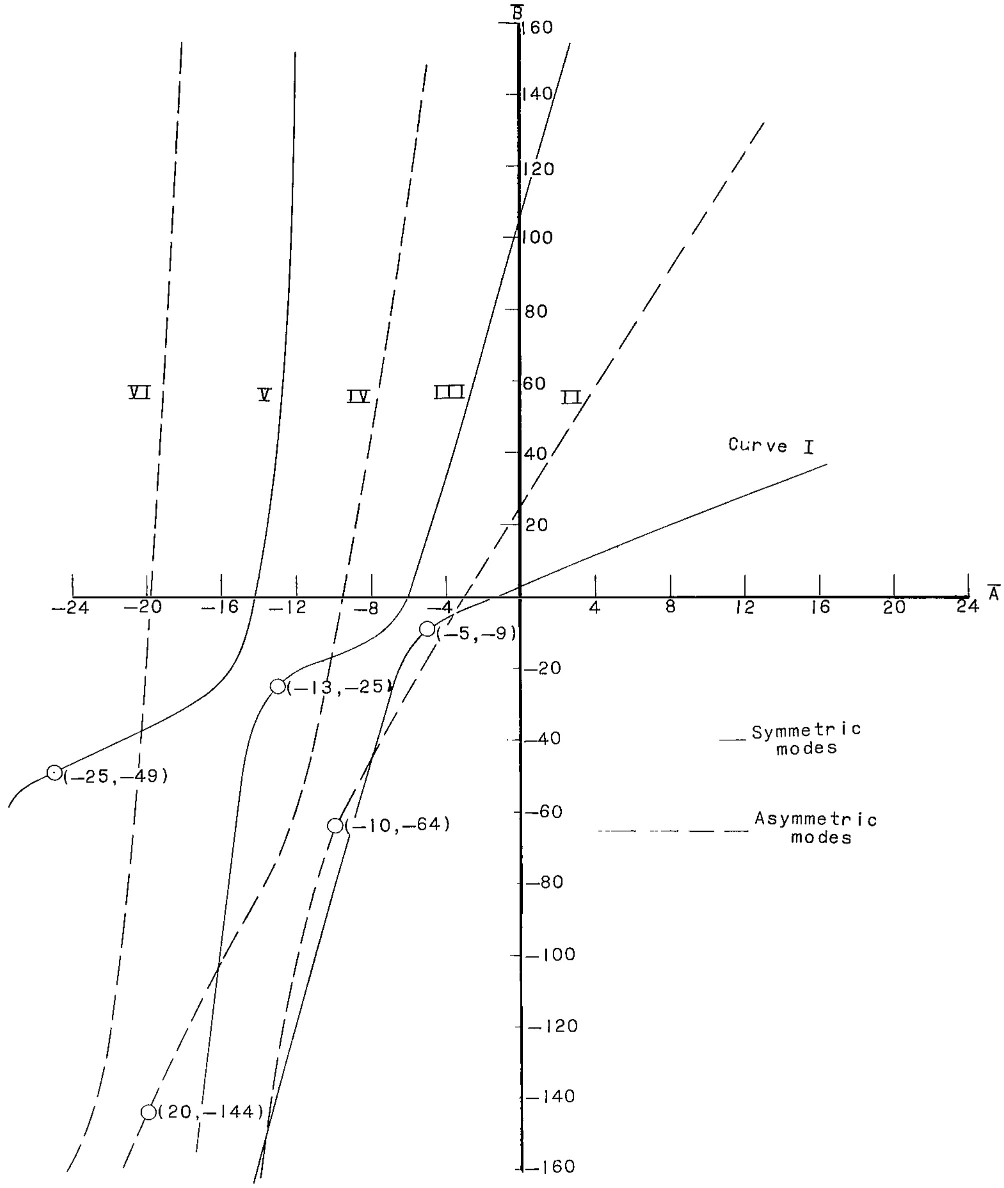

Figure 4.- Variation of $\bar{B}$ with $\bar{A}$ for plate elastically restrained on boundaries $x = \pm\frac{a}{2}$. $q_x = 10$.

Linear interpolation within the tables may be used for values of $\bar{A}$ and $\bar{B}$ not tabulated. For values of positive $\bar{A}$ greater than those presented in the tables, the corresponding values of $\bar{B}$ can be determined from the approximate equation (A8) derived in appendix A. This equation becomes more accurate as $\bar{A} \rightarrow \infty$. No values of $\bar{A}$ and $\bar{B}$ were tabulated for $q_x = 0$ as these values are readily obtained from equation (21). For values of q_x not used in the solutions of the frequency equations, the corresponding values of $\bar{A}$ and $\bar{B}$ can be obtained by cross plotting the results in the tables.

Modal Characteristics

For simple support boundary conditions, the mode shapes (eq. (20)) are exact solutions regardless of the inplane loading condition. Hence the mode shapes for simply supported plates are independent of inplane stress. This independence results in a linear $\bar{A},\bar{B}$ relation given by equation (21) and plotted in figure 2. In contrast, for boundary conditions other than simple supports the mode shapes given by equations (18) and (19) are dependent on α and β or $\bar{\beta}$ which are functions of $\bar{A}$ and $\bar{B}$ (eqs. (12) and (15)). This dependence of mode on stress results in nonlinear $\bar{A},\bar{B}$ relations as shown in figures 3 and 4. For the range of $\bar{A}$ where the variation of $\bar{B}$ with $\bar{A}$ is nearly linear, the changes in mode shape with stress are slight. For the range of $\bar{A}$ for which the $\bar{B},\bar{A}$ variations are highly nonlinear, the changes in mode shape with stress are significant. An example showing the change in symmetrical mode shapes for clamped supports is illustrated in figure 5 by plotting mode shapes corresponding to various values of $\bar{A}$ and $\bar{B}$. The $\bar{A},\bar{B}$ plot is divided into three regions by the $\bar{B} = 0$ line and the curves for the first and third simply supported modes. In these regions each curve has a characteristic mode shape as shown in figure 5. For instance, consider curve III_m, where the subscript m indicates the mode number. In region R along the III_3 curve, two node lines exist. From the $\bar{B} = 0$ line to the first simply supported mode line, or region R_1, no node lines exist along the III_1 curve. Between the first and third simply supported mode lines, or region R_3, two node lines again exist along the III_3 curve. Generalizing, for negative $\bar{B}$, it is found that the first mode $(m = 1)$ can exist only in region R_1. (Note that while no points of zero deflection exist in region R_1, hence no node lines, the mode shapes may have more than one point of inflection.) Similarly, the third mode $(m = 3)$ can exist only in the region of $\bar{B}$ (region R_3) defined between the first and third simply supported modes; the fifth mode can exist only in the region of $\bar{B}$ defined between the third and fifth simply supported modes; and so on.

Similar behavior is also observed for the clamped asymmetrical modes as well as for the symmetrical and asymmetrical modes with rotational restraint. Further, it is noted that certain solutions to the frequency equations are independent of the magnitude of rotational restraint. These points are indicated in figures 2 to 5 by the circles and correspond to points of a change in mode number for $q_x > 0$.

With the preceding observations it was found that the modal characteristics of an orthotropic plate can be described as follows: for $\bar{B}$ negative, if m is odd (even), all symmetrical (asymmetrical) modes, for clamped or rotationally restrained supports, between the mth and $m - 2$ simply supported modes can exist only in the mth mode. (The cases of $m - 2 = -1$ for $m = 1$ and $m - 2 = 0$ for $m = 2$ should be interpreted as the $\bar{B} = 0$ axis.)

With this modal behavior, which is typical of what has been presented, it is interesting to note that, for $q_x > 0$, the first (fundamental) mode (as

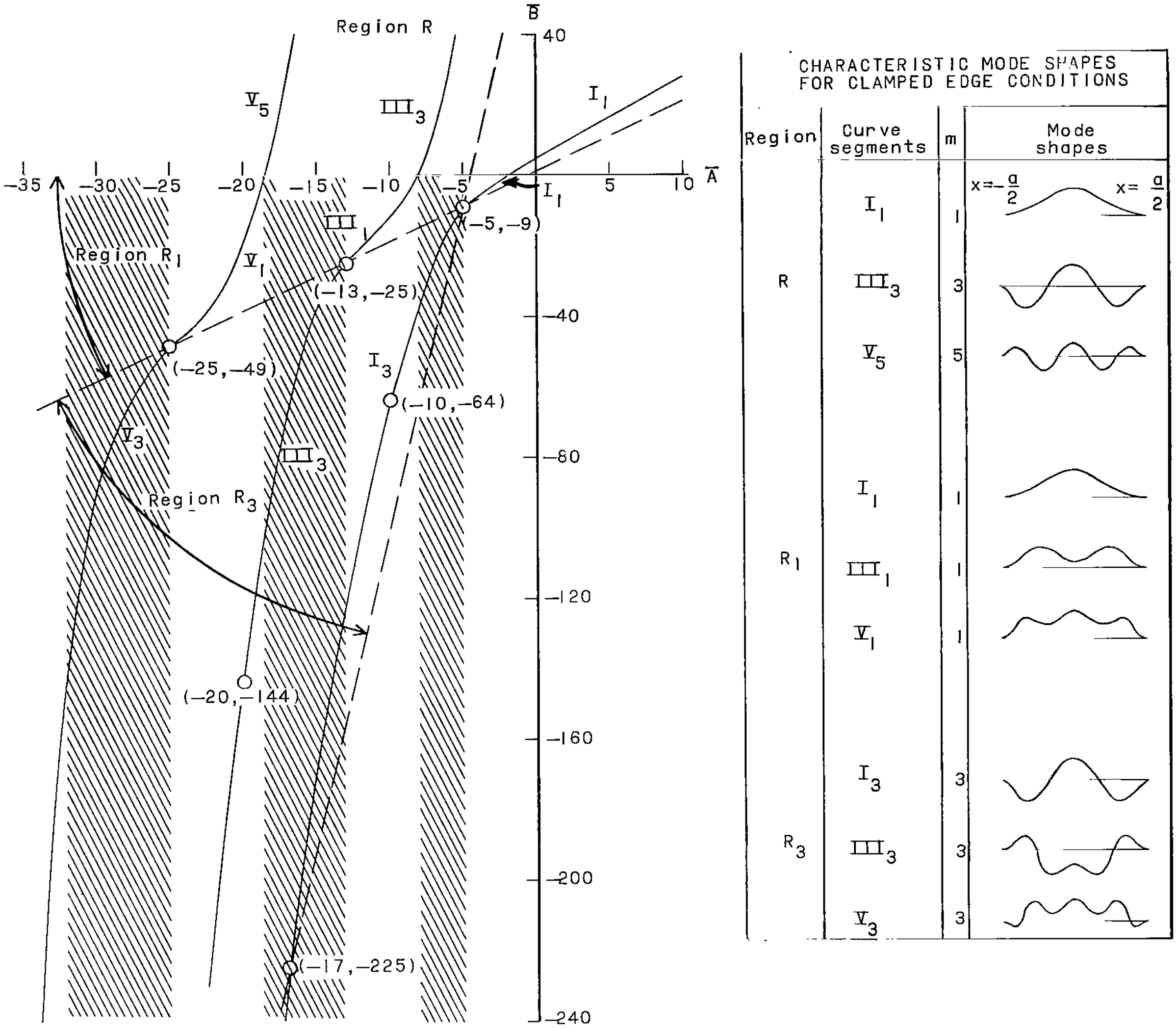

Figure 5.- Variation of $\bar{B}$ with $\bar{A}$ for symmetrical modes for clamped and simple supports showing regions of existence of mode shapes. Shaded areas indicate absence of first mode.

defined herein) does not exist for certain values of negative $\bar{A}$. These regions are indicated by the shaded areas in figure 5 for clamped supports.

It should be further noted that, from the definition of $\bar{A}$ and $\bar{B}$ (eq. (4)), a necessary requirement to be in the negative $\bar{A},\bar{B}$ region is compressive inplane loading in the x-direction. (When the inplane loading becomes compressive, the increasing order of frequencies does not necessarily correspond to an increasing order of mode numbers.)

Application of Results

In the preceding sections, the results have been discussed in terms of the general parameters $\bar{A}$ and $\bar{B}$. The application of these results to obtain the natural frequencies of a rectangular plate subjected to normal inplane loadings and having arbitrary rotational restraint at the edges is illustrated in the following sections. The buckling load may also be determined by setting the frequency equal to zero. Without restricting the generality of the results, the following numerical examples will be given only for an isotropic plate, that is, $D_1 = D_{12} = D_2 = D$.

For any given problem the orientation of the coordinate system is arbitrary (the x- and y-coordinates of fig. 1 may be interchanged) for the calculation of C_1/C_0 and C_2/C_0 and finally, $\bar{A}$ and $\bar{B}$. The preferred orientation is the one that leads to the lowest buckling load or vibration frequency since this load or frequency corresponds more closely to the exact answer. As a guide, if at least one value of $\bar{A}$ calculated from both orientations is negative, the orientation giving the largest negative $\bar{A}$ should be used. If both values of $\bar{A}$ are positive, the orientation giving the largest positive $\bar{A}$ should be used. This procedure is followed in the calculations of the following examples.

Effect of inplane stress on natural frequency.- For a beam, $\bar{A}$ and $\bar{B}$ reduce to a nondimensional axial load and frequency, respectively, so the tabulated solutions for $\bar{B}$ positive give the frequency-stress relations directly. However, the coefficients C_1/C_0 and C_2/C_0 in the parameters $\bar{A}$ and $\bar{B}$ for a plate are functions of the mode shape in the y-direction. Clearly then, the values of these coefficients, and hence, the support conditions on the $y = \pm\frac{b}{2}$ boundaries must be specified before the frequency-stress relationship of a plate can be determined. In appendix B, a method of calculating these coefficients using beam modes is given for values of rotational restraint $0 \leqq q_y \leqq \infty$. The results for the first four modes are plotted in figures 6 and 7. With C_1/C_0 and C_2/C_0 known for any rotational elastic restraint, and q_y and a/b given, $\bar{A}$ can be calculated for any k_x. Then, with the appropriate boundary conditions

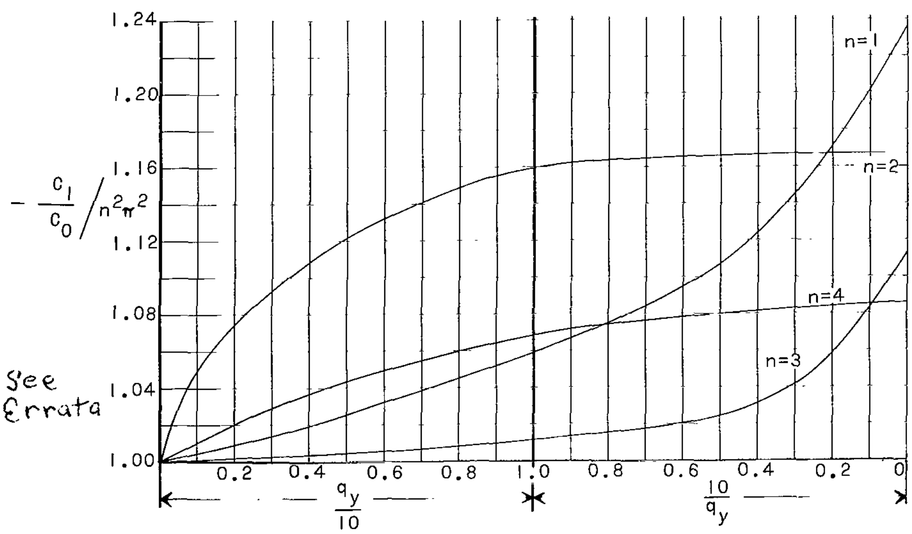

Figure 6.- Variation of C_1/C_0 with rotational restraint coefficient q_y for first four modes in y-direction.

at $x = \pm\frac{a}{2}$, the corresponding value of $\overline{B}$ can be obtained from the tables and hence, the frequency $\left(\frac{\omega}{\omega_o}\right)^2$ can be calculated for any k_y.

The results of this procedure are shown in figure 8 for (a) a plate simply supported on all four edges and (b) a plate clamped at the edges $x = \pm\frac{a}{2}$ and simply supported at the edges $y = \pm\frac{b}{2}$. The results are exact since the edges are simply supported at $y = \pm\frac{b}{2}$. From figures 6 and 7,

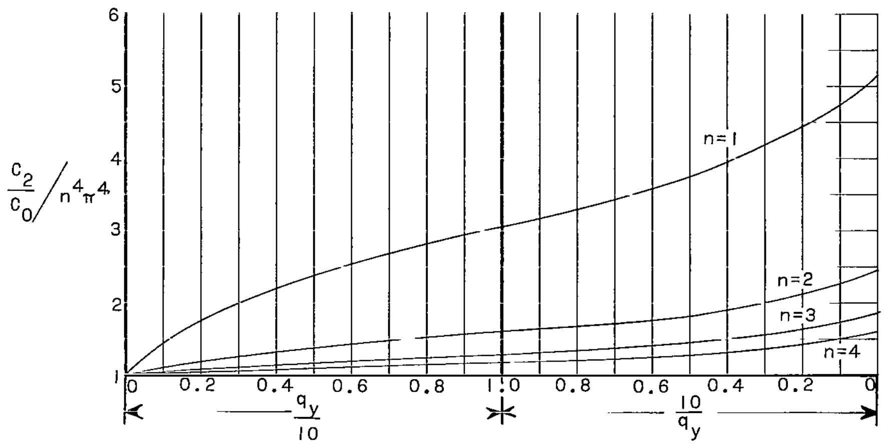

Figure 7.- Variation of C_2/C_0 with rotational restraint coefficient q_y for first four modes in y-direction.

$\frac{C_1}{\pi^2 C_0} = -1$ and $\frac{C_2}{C_0\pi^4} = 1$, hence, $\overline{A}$ and $\overline{B}$ become (see eq. (4))

$$\left.\begin{aligned} \overline{A} &= +\left(\frac{a}{b}\right)^2\left(n^2 - \frac{k_x}{2}\right) \\ \overline{B} &= \left(\frac{\omega}{\omega_o}\right)^2 - n^2\left(\frac{a}{b}\right)^4\left(n^2 - k_y\right) \end{aligned}\right\} \tag{22}$$

where a/b, n, and k_y were arbitrarily chosen to be $\frac{a}{b} = 3$, $n = 1$, and $k_y = 0$.

Figure 8 shows that an increase in stress results in a linear decrease in the square of the frequency for the simply supported plate but a nonlinear decrease for the plate clamped along the loaded edges. Also shown in the figure is the region of absence of the first mode (for the case where the loaded edges were clamped) along with the points $\overline{A},\overline{B}$ where the mode numbers change. For correlation of these $\overline{A},\overline{B}$ points, see figures 2 and 3.

Plate buckling characteristics.- The buckling stress for a plate with given geometry and boundary conditions can be determined from the frequency-stress plot for the plate as the lowest stress which makes a zero frequency. However, it is more suitable to use the solutions in terms of $\overline{A}$ and $\overline{B}$ directly. For buckling, with a given value of $\overline{A}$, the curve (see, for instance, figs. 2 to 4) with the lowest value of $\overline{B}$ should be used to obtain the lowest buckling load. For illustration, the previous example of a plate simply supported at $y = \pm\frac{b}{2}$ and clamped at $x = \pm\frac{a}{2}$ will be considered. With $\left(\frac{\omega}{\omega_o}\right)^2 = 0$, equation (22) yields

$$\left.\begin{aligned}\bar{A} &= -\left(\frac{a}{b}\right)^2\left(-n^2 + \frac{k_x}{2}\right)\\ \bar{B} &= -\left(\frac{a}{b}\right)^4\left(n^4 - n^2k_y\right)\end{aligned}\right\} \tag{23}$$

With k_y specified, the variation of k_x with $\frac{a}{b}$ can be determined for specified values of n for the values of $\bar{A}$ and $\bar{B}$ (table 1) which satisfy the

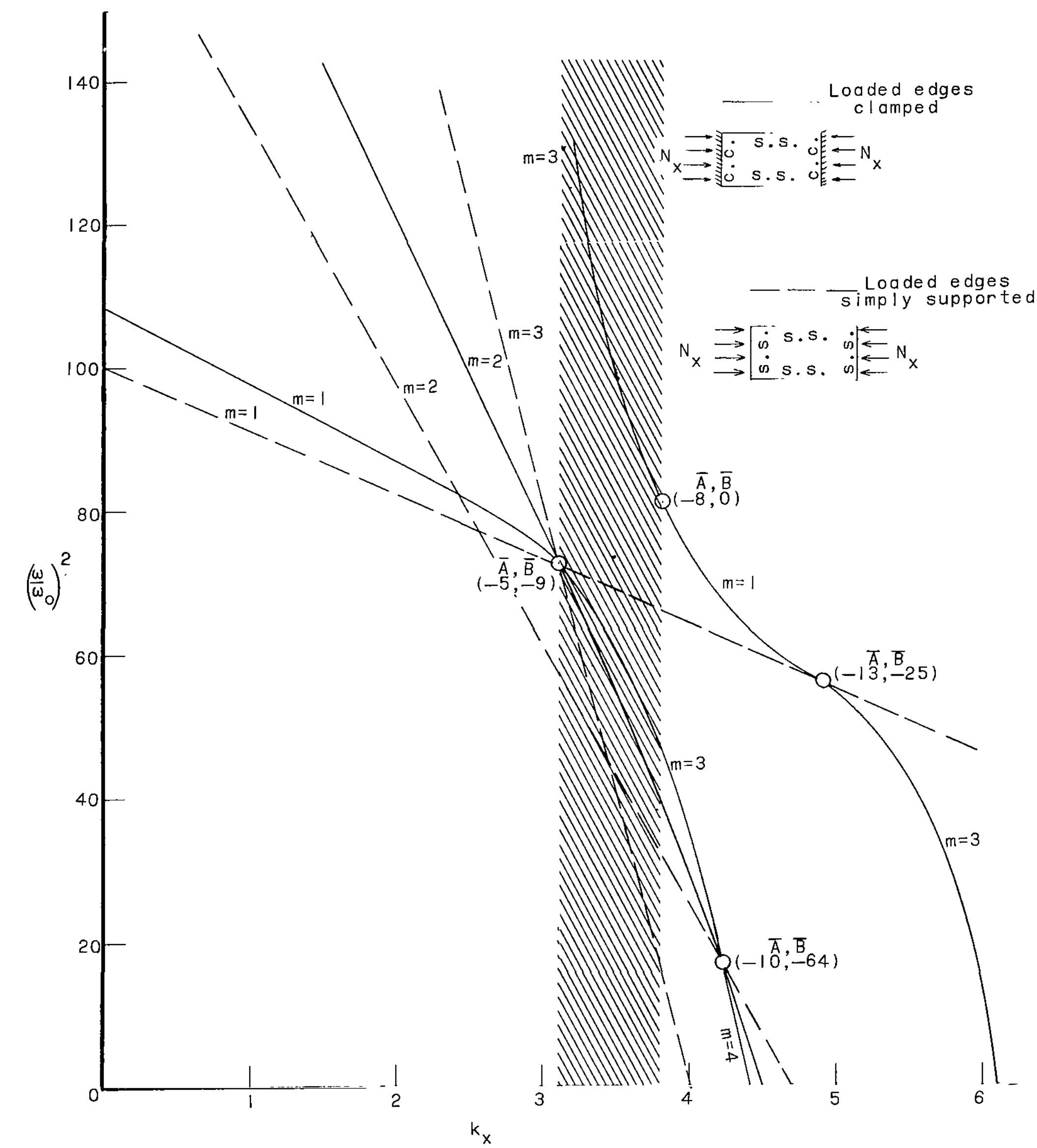

Figure 8.- Variation of frequency parameter with stress coefficient for a clamped and simply supported plate at $x = \pm\frac{a}{2}$. $\frac{a}{b} = 3$; $k_y = 0$; $n = 1$. Shaded area indicates absence of first mode.

frequency equations (16) and (17). The appropriate value of n is that which yields the lowest value of k_x. The results obtained from equation (23) for $k_y = 0$, for which $n = 1$, are shown in figure 9; also shown for comparison are the approximate solutions of reference 14.

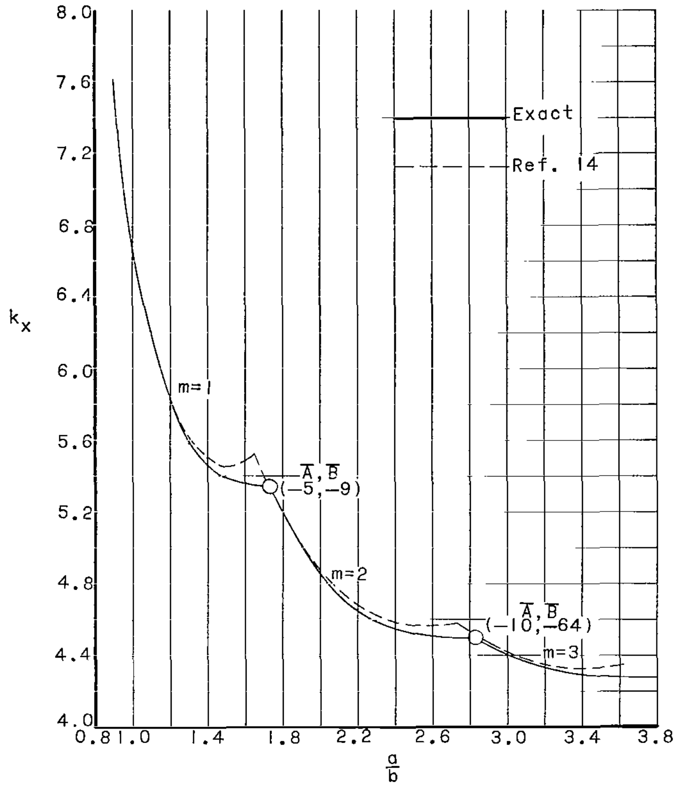

Figure 9.- Nondimensional buckling stress plotted against $\frac{a}{b}$ for plate clamped at $x = \pm\frac{a}{2}$ simply supported at $y = \pm\frac{b}{2}$. $k_y = 0$; $n = 1$.

Comparison With Other Results

The preceding examples are exact because one pair of opposite edges was simply supported. An indication of the accuracy of the approximate results can be obtained by considering a case where all edges are rotationally restrained. One of the largest deviations from the exact solution could be expected for a square plate clamped on all four edges since the edge effects (boundary conditions) are more predominant than they are for other length-width ratios. Accordingly, the vibration and buckling characteristics of such a plate have been determined by the method presented herein for comparison with the results which have been obtained in the literature.

Comparison with converged series solutions.- The case of a square clamped plate loaded in uniform tension along all four edges with $k_x = k_y = -10$ is considered in reference 8. With a series representation of the panel deflection, convergence was established with six modes in each direction that resulted in a value of $\left(\frac{\omega}{\omega_o}\right)^2 = 36.94$ for the fundamental frequency ($m = n = 1$). To use the method in the present paper, refer to figures 6 and 7 to determine C_1/C_0 and C_2/C_0. Then $\bar{A}$ and $\bar{B}$ become (see eq. (4))

$$\left.\begin{aligned} \bar{A} &= 1.235 + 5 = 6.235 \\ \bar{B} &= -5.14 - 12.35 + \left(\frac{\omega}{\omega_o}\right)^2 = -17.49 + \left(\frac{\omega}{\omega_o}\right)^2 \end{aligned}\right\} \tag{24}$$

Linear interpolation from table 1(a) gives the lowest value of $\bar{B}$ for the given $\bar{A}$ as $\bar{B} = 19.93$. Hence $\left(\frac{\omega}{\omega_0}\right)^2 = 37.42$. Thus the error of the method in the present paper is only 1.3 percent.

In reference 15 the buckling of a square plate loaded in compression along two opposite edges is considered. On the basis of computations involving determinants up to the twentieth order, the solution obtained was $k_x(\text{critical}) = 10.08$ for $m = n = 1$. To use the method of the present paper, again refer to figures 6 and 7 to determine C_1/C_0 and C_2/C_0. Then $\bar{A}$ and $\bar{B}$ become (see eq. (4))

$$\left.\begin{aligned} \bar{A} &= -\left(-1.235 + \frac{k_x}{2}\right) \\ \bar{B} &= -5.14 \end{aligned}\right\} \qquad (25)$$

The lowest value of $\bar{A}$ for the given $\bar{B}$ is found by interpolation from table 1(a) to be $\bar{A} = -3.82$. Hence $k_x(\text{critical}) = 10.12$. Thus, the error of the method of the present paper is 0.4 percent of a result obtained by a much more laborious method.

Finally, in reference 2 frequency results are given for several modes of a square clamped plate with no inplane load. It was assumed that convergence was obtained with a 36-term series. The results are given in the following table and are compared with results obtained by the method of the present paper:

Source	$(\omega/\omega_0)^2$ for -			
	$m = 1$, $n = 1$	$m = 1$, $n = 2$	$m = 2$, $n = 2$	$m = 2$, $n = 3$
Reference 2	13.30	55.32	120.3	280.0
Present paper	13.32	55.64	120.6	279.8
Percent variation . . .	0.15	0.58	0.25	0.072

From these comparisons it is seen that the method of the present paper is very accurate for a square clamped plate. For other length-width ratios and boundary conditions the accuracy would be expected to be as good or better. Thus the results tabulated in tables 1 to 4 provide an accurate and rapid means of calculating the frequencies and buckling loads of plates for large ranges of length-width ratio, stiffness ratio, inplane loading, and boundary conditions.

Comparison with approximate solutions.- The methods of Galerkin (ref. 13) or Ritz (ref. 2) are often used to obtain approximate solutions to the differential equation (1a) directly. For a plate clamped on all edges, application of the Galerkin or Ritz procedure using a single clamped beam mode in each

direction (integrals are tabulated in refs. 16 and 17) results in the following linear $\bar{A},\bar{B}$ relations for the first four modes

$$\left.\begin{aligned} m = 1:&\quad -\bar{B} + 2.47\bar{A} + 5.14 = 0 \\ m = 2:&\quad -\bar{B} + 9.33\bar{A} + 39.05 = 0 \\ m = 3:&\quad -\bar{B} + 20.04\bar{A} + 150 = 0 \\ m = 4:&\quad -\bar{B} + 34.77\bar{A} + 410.06 = 0 \end{aligned}\right\} \tag{26}$$

where $\bar{A}$ and $\bar{B}$ are as defined previously. Results from equations (26) are plotted in figure 10 for comparison with the results of the present method. It can be seen that these results are in good agreement with the present solution in the negative $\bar{B}$ region only for a limited range of $\bar{A}$. This range of $\bar{A}$ could be extended, of course, if more modes were used in the analysis. (See, for example, ref. 18.) Similar agreement can be found for finite values of q_x.

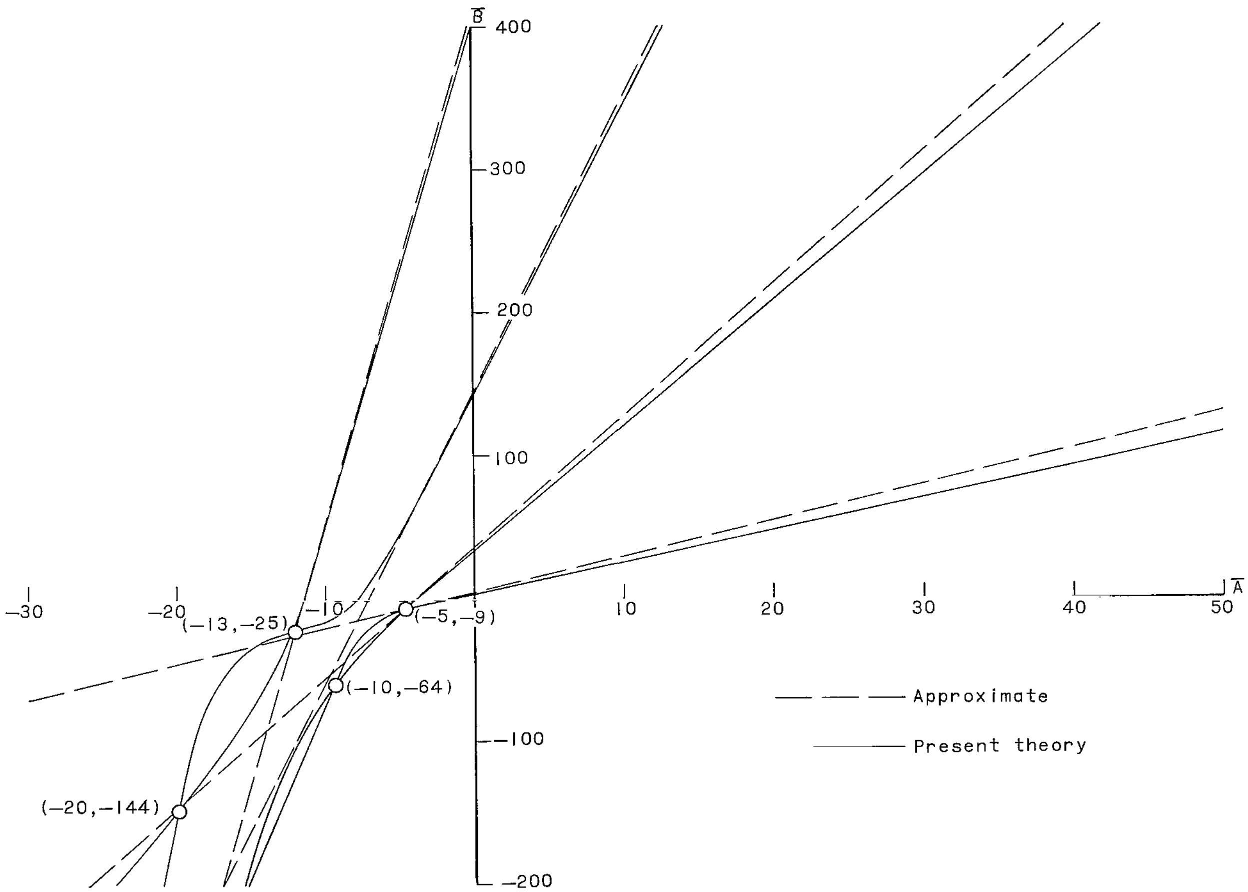

Figure 10.- Comparison of $\bar{A},\bar{B}$ relations obtained from present theory and one-term Galerkin solutions for clamped supports at $x = \pm\frac{a}{2}$.

CONCLUDING REMARKS

The natural vibration and buckling characteristics of flat orthotropic rectangular plates with uniform inplane loads and various rotational restraints at the boundaries have been examined theoretically. The governing partial differential equation for small deflections was reduced to an ordinary differential equation by assuming an approximate mode shape in one direction. Beam modes were used and the boundary conditions were satisfied. The differential equation was solved exactly and the boundary conditions were applied to obtain a set of frequency equations valid for any degree of rotational restraint. These frequency equations were solved in terms of two general parameters $\bar{A}$ and $\bar{B}$ which are functions of inplane stress, length-width ratio, frequency, stiffness ratios, and the assumed mode shape. Values of $\bar{A}$ and $\bar{B}$ which satisfy the frequency equations are tabulated for modes with up to five node lines in one direction and any number in the other, from which the buckling and vibration characteristics of an orthotropic rectangular plate can be quickly determined for any combination of inplane loading and boundary rotational restraint. The accuracy of this assumed-mode approximation is indicated by comparison with converged modal results for a square clamped plate. The buckling load differed from the converged results by 0.4 percent. For a plate with large inplane tension the first natural frequency differed from the converged results by 1.3 percent and by 0.15 percent for a plate without inplane stress. For other boundary conditions and length-width ratios the differences are expected to be no greater and in many cases will be less. Thus the tabulated results provide an accurate and rapid means of calculating the frequencies and buckling loads of plates for large ranges of length-width ratio, stiffness ratio, inplane loading, and boundary conditions.

Other results of the investigation revealed:

1. The square of the frequency is a linear function of inplane stress for simply supported plates but may be nonlinear for plates with other edge conditions.

2. The fundamental mode does not exist for certain ranges of compressive loading unless all loaded edges are simply supported.

3. The one-term Galerkin solutions and Ritz solutions often used for vibrating plate problems can be considerably in error for certain values of compressive loading and plate length-width ratio.

Langley Research Center,
National Aeronautics and Space Administration,
Langley Station, Hampton, Va., February 9, 1965.

APPENDIX A

APPROXIMATE SOLUTIONS OF THE FREQUENCY EQUATIONS

An approximate relation is developed herein which may be used to determine values of $\overline{B}$ for any given value of $\overline{A}$ greater than that presented in the tables. This approximation becomes exact as $\overline{A} \to \infty$.

Consider the first of the frequency equations (16) rewritten here for convenience as

$$\frac{1}{q_x}\left(2\alpha^2 + 2\beta^2\right) + (\alpha \tan \alpha + \beta \tanh \beta) = 0 \tag{A1}$$

Note that as $\alpha \to \frac{m\pi}{2}$ where m is odd, $\beta \to \infty$ and $\tanh \beta \to 1$, hence $\overline{A} \to \infty$ (see eq. 4). For this case, an approximate relation between $\overline{A}$ and $\overline{B}$ can be obtained as follows: Let

$$\alpha = \epsilon + \frac{m\pi}{2} \tag{A2}$$

where ϵ is some vanishingly small positive number and hence, $\tan \alpha$ is a negative number, that is

$$\tan\left(\epsilon + \frac{m\pi}{2}\right) \approx -\frac{1}{\epsilon} \tag{A3}$$

Substitution of equations (A2) and (A3) into equation (A1) gives

$$-\frac{1}{q_x}\left(2\alpha^2 + 2\beta^2\right) + \frac{\epsilon + \frac{m\pi}{2}}{\alpha - \frac{m\pi}{2}} - \beta = 0 \tag{A4}$$

It is convenient to write this equation in the following form

$$\alpha = \frac{\epsilon + \frac{m\pi}{2}}{\beta + \frac{1}{q_x}\left(2\alpha^2 + 2\beta^2\right)} + \frac{m\pi}{2} \tag{A5}$$

Substitution of equation (A2) into the first of equations (12) gives

$$\beta = \sqrt{\frac{\pi^2\overline{A}}{2} + \epsilon^2 + \epsilon m\pi + \frac{m^2\pi^2}{4}} \tag{A6}$$

From the second of equations (12)

$$\bar{B} = \frac{16}{\pi^4}\alpha^2\beta^2 \tag{A7}$$

If equations (A5) and (A6) are substituted into equation (A7) and ϵ is allowed to approach zero, the result is

$$\bar{B} = \left(2\bar{A}m^2 + m^4\right)\left[\frac{1}{\frac{\pi}{2}\sqrt{2A + m^2} + \frac{\pi^2}{q_x}\left(\bar{A} + m^2\right)} + 1\right]^2 \tag{A8}$$

Thus, for any given value of $\bar{A}$ and q_x, the corresponding value of $\bar{B}$ can be calculated. It is emphasized again, however, that this relation should be used only for positive values of $\bar{B}$ greater than those listed in the tables.

Use of equation (A2) in the second of equations (16) with m even gives the same results as equation (A8). Hence, equation (A8) can be used for both the symmetrical and the asymmetrical modes. Further, equation (A8) shows the interesting relationship that when $\bar{B}$ attains large positive values, the value of $\bar{B}$ for $q_x \neq 0$ is the value of $\bar{B}$ for simple supports ($q_x = 0$) plus some additional parameter which takes into account the effect of the edge restraints.

APPENDIX B

DERIVATION OF COEFFICIENTS C_1/C_0 AND C_2/C_0

The deflection functions, $Y(\eta)$, used to determine the coefficients C_1/C_0 and C_2/C_0 must satisfy the boundary conditions.

Clamped beam modes give good results for $q_x = \infty$ with $\bar{A} \approx 0$ and $\bar{B}$ positive (see fig. 10) and, thus, the beam modes for each finite q_y will be assumed to give satisfactory results for the calculation of C_1/C_0 and C_2/C_0. These beam modes can be obtained from the equations already derived (eq. (18)) by letting $\frac{a}{b} \rightarrow 0$. Further, for no axial load, $\bar{A} = 0$, which implies $\alpha = \beta$ (see eq. (12)). Thus, C_1/C_0 can be written as a function of one parameter, say δ, where δ is a function of q_y. Use of the mode shapes as given by equation (18) in equation (7) gives the coefficients C_1/C_0 and C_2/C_0

$$\left.\begin{aligned}
\left(\frac{C_1}{C_0}\right)_S &= 4\delta^2\left[\frac{-1 + \cos^2\delta\left(\frac{4}{q_y} + 1 + \frac{2\tanh\delta}{\delta} - \tanh^2\delta\right)}{1 + \cos^2\delta\left(\frac{4}{q_y} + 1 - \tanh^2\delta\right)}\right] && \text{(Symmetrical)} \\
\text{See Errata}\quad\left(\frac{C_1}{C_0}\right)_A &= 4\delta^2\left[\frac{-1 + \sin^2\delta\left(\frac{4}{q_y} + 1 + \frac{2}{\delta\tanh\delta} - \frac{1}{\tanh^2\delta}\right)}{1 + \sin^2\delta\left(-\frac{4}{q_y} + 1 - \frac{1}{\tanh^2\delta}\right)}\right] && \text{(Asymmetrical)}
\end{aligned}\right\} \quad \text{(B1)}$$

$$\left.\begin{aligned}
\left(\frac{C_2}{C_0}\right)_S &= 16\delta^4 && \text{(Symmetrical)} \\
\left(\frac{C_2}{C_0}\right)_A &= 16\delta^4 && \text{(Asymmetrical)}
\end{aligned}\right\} \quad \text{(B2)}$$

For $q_y = 0$ (simple supports), these equations reduce to

$$\frac{C_1}{C_0} = -n^2\pi^2 \qquad \frac{C_2}{C_0} = n^4\pi^4$$

which are exact for both the symmetrical and the asymmetrical modes.

APPENDIX B

With equations (B1) and (B2), the variation of C_1/C_0 and C_2/C_0 with q_y for each mode can be calculated. The results are plotted in figures (6) and (7) using the data of table 5. With these curves, and tables 1 to 4, the vibration and buckling characteristics of an orthotropic plate with any combination of clamped and/or rotational restraints can now be determined.

REFERENCES

1. Warburton, G. B.: The Vibration of Rectangular Plates. Proc. Inst. Mech. Eng. (London), vol. 168, no. 12, 1953, pp. 371-384.

2. Young, Dana: Vibration of Rectangular Plates by the Ritz Method. J. Appl. Mech., vol. 17, no. 4, Dec. 1950, pp. 448-453.

3. Timoshenko, S.: Vibration Problems in Engineering, 3rd ed., D. Van Nostrand Co., Inc., 1955, p. 443.

4. Langhaar, Henry L.: Energy Methods in Applied Mechanics. John Wiley & Sons, Inc., c.1962.

5. Lurie, Harold: Lateral Vibrations as Related to Structural Stability. J. Appl. Mech. vol. 19, no. 2, June 1952, pp. 195-204.

6. Herrmann, George: The Influence of Initial Stress on the Dynamic Behavior of Elastic and Viscoelastic Plates. Reprint from Intern. Assoc. Bridge Structural Eng. Publ., vol. 16, 1956, pp. 275-294.

7. Nowacki, Witold (Henryk Zorski, trans.): Dynamics of Elastic Systems. John Wiley & Sons, Inc., 1963.

8. Kaul, R. K.; and Tewari, S. G.: On the Bounds of Eigenvalues of a Clamped Plate in Tension. J. Appl. Mech., vol. 25, no. 1, Mar. 1958, pp. 52-56.

9. Weinstein, Alexander; and Chien, Wei Zang: On the Vibration of a Clamped Plate Under Tension. Quart. Appl. Math., vol. I, no. 1, April 1943, pp. 61-68.

10. Trubert, Marc; and Nash, William A.: Effect of Membrane Forces on Lateral Vibrations of Rectangular Plates. Tech. Note No. 2 (AFOSR TN-60-437), Eng. Ind. Exptl. Sta., Univ. of Florida, May 1960.

11. Shulman, Yechiel: On the Vibration of Thermally Stressed Plates in the Pre-Buckling and Post-Buckling States. Tech. Rept. 25-25, Office of Naval Res., Jan. 1958.

12. Libove, C.; and Batdorf, S. B.: A General Small-Deflection Theory for Flat Sandwich Plates. NACA Rept. 899, 1948. (Supersedes NACA TN 1526.)

13. Kantorovich, L. V.; and Krylov, V. I. (Curtis D. Benster, trans.): Approximate Methods of Higher Analysis. Interscience Publ. 1958.

14. Libove, Charles; and Stein, Manuel: Charts for Critical Combinations of Longitudinal and Transverse Direct Stress for Flat Rectangular Plates. NACA WR L-224, 1946. (Formerly NACA ARR L6A05.)

15. Levy, Samuel: Buckling of Rectangular Plates With Built-in Edges. J. Appl. Mech., vol. 9, no. 4, Dec. 1942, pp. A-171 - A-174.

16. Young, Dana; and Felgar, Robert P., Jr.: Tables of Characteristic Functions Representing Normal Modes of Vibration of a Beam. Pub. No. 4913, Eng. Res. Ser. No. 44, Bur. Eng. Res., Univ. of Texas, July 1, 1949.

17. Felgar, Robert P., Jr.: Formulas for Integrals Containing Characteristics Functions of a Vibrating Beam. Circ. No. 14, Bur. Eng. Res., Univ. of Texas, 1950.

18. Dixon, Sidney C.: Application of Transtability Concept to Flutter of Finite Panels and Experimental Results. NASA TN D-1948, 1963.

TABLE 1.- SOLUTIONS OF FREQUENCY EQUATIONS IN TERMS OF $\bar{A}$ AND $\bar{B}$ FOR CLAMPED SUPPORTS WITH $q_x = \infty$

(a) Symmetrical modes

$\bar{A}$	$\bar{B}$	$\bar{A}$	$\bar{B}$	$\bar{A}$	$\bar{B}$	$\bar{A}$	$\bar{B}$	$\bar{A}$	$\bar{B}$	$\bar{A}$	$\bar{B}$	$\bar{A}$	$\bar{B}$	$\bar{A}$	$\bar{B}$
Curve I															
(1)*		-2	0	(3)		-10.23	-68.57	(5)		-26.45	-599.5	(7)		-50.67	-2371
+∞	+∞	-2.005	-.0124	-5.560	-11.15	-10.46	-73.40	-17.63	-242.1	-26.91	-623.9	-37.83	-1280	-51.35	-2441
72.23	162.2	-2.019	-.0497	-6.008	-13.51	-10.71	-78.52	-18.27	-259.9	-27.38	-649.2	-38.65	-1337	-52.04	-2512
19.24	49.02	-2.042	-.1127	-6.543	-15.96	-10.97	-83.96	-18.88	-278.2	-27.86	-675.5	-39.47	-1395	-52.75	-2586
8.798	25.80	-2.076	-.2026	-6.923	-18.45	-11.24	-89.75	-19.48	-296.7	-28.36	-703.0	-40.28	-1453	-53.47	-2662
4.892	16.85	-2.120	-.3212	-7.241	-20.98	-11.53	-95.93	-20.05	-315.4	-28.87	-731.8	-41.07	-1512	-54.21	-2740
2.940	12.27	-2.176	-.4712	-7.514	-23.56	-11.84	-102.6	-20.59	-334.1	-29.41	-761.9	-41.83	-1571	-54.97	-2822
1.785	9.506	-2.245	-.6560	-7.757	-26.20	-12.17	-109.7	-21.10	-352.9	-29.97	-793.6	-42.58	-1630	-55.75	-2906
1.017	7.646	-2.328	-.8805	-7.979	-28.94	-12.51	-117.4	-21.60	-371.7	-30.54	-827.0	-43.31	-1689	-56.56	-2994
.4638	6.288	-2.427	-1.151	-8.187	-31.78	-12.89	-125.7	-22.07	-390.6	-31.15	-862.2	-44.01	-1748	-57.39	-3086
.0379	5.233	-2.546	-1.476	-8.387	-34.75	-13.29	-134.7	-22.52	-409.7	-31.78	-899.4	-44.71	-1807	-58.25	-3182
-.3066	4.371	-2.688	-1.869	-8.583	-37.82	-13.72	-144.5	-22.97	-429.0	-32.44	-938.8	-45.38	-1867	-59.14	-3282
-.5967	3.640	-2.859	-2.344	-8.776	-41.04	-14.18	-155.2	-23.41	-448.6	-33.13	-980.5	-46.05	-1926	-60.06	-3386
-.8493	2.998	-3.066	-2.926	-8.970	-44.42	-14.68	-166.9	-23.84	-468.5	-33.86	-1025	-46.71	-1987	-61.01	-3494
-1.075	2.149	-3.318	-3.649	-9.167	-47.95	-15.21	-179.8	-24.27	-488.9	-34.61	-1071	-47.37	-2048	-61.97	-3607
-1.282	1.886	-3.628	-4.556	-9.366	-51.67	-15.78	-193.7	-24.69	-509.8	-35.38	-1120	-48.02	-2110	-62.96	-3724
-1.474	1.385	-4.008	-5.709	-9.571	-55.57	-16.38	-208.8	-25.12	-531.2	-36.18	-1172	-48.68	-2174	-63.97	-3845
-1.659	.9087	-4.469	-7.176	-9.782	-59.67	-17	-225	-25.56	-553.3	-37	-1225	-49.34	-2238	-65	-3969
-1.831	.4487	-5	-9	-10	-64			-26	-576			-50	-2304		
Curve III															
(3)		-7.238	9.793	-9.522	-11.15	-18.78	-96.60	-23.50	-273.9	-35.48	-701.2	-42.92	-1259	-56.46	-2302
+∞	+∞	-7.646	4.134	-9.992	-13.40	-18.97	-103.7	-24.02	-291.1	-36.01	-731.8	-43.45	-1304	-57.52	-2393
605.2	11390	-8	0	-10.67	-16.24	-19.17	-111.2	-24.62	-310.1	-36.48	-762.5	-44.07	-1351	-58.51	-2484
150.8	3013	(1)		-11.66	-20.01	-19.37	-118.9	-25.30	-330.9	-36.94	-793.5	-44.70	-1400	-59.43	-2572
64.82	1401	-8.004	-.0124	-13	-25	-19.57	-126.9	-26.08	-354.3	-37.39	-824.7	-45.38	-1453	-60.30	-2659
33.99	813.7	-8.019	-.1978	(3)		-19.78	-135.3	-26.96	-380.4	-37.83	-856.3	-46.10	-1508	-61.12	-2745
19.33	530.9	-8.042	-.4460	-14.40	-30.85	-20	-144	-27.95	-409.4	-38.26	-888.5	-46.88	-1568	-61.89	-2829
11.11	370.4	-8.076	-.7952	-15.49	-36.73	-20.23	-153.1	-29	-441	-38.69	-921.2	-47.73	-1631	-62.62	-2913
5.970	269.0	-8.121	-1.247	-16.24	-42.35	-20.46	-162.5	(5)		-39.12	-954.7	-48.65	-1700	-63.33	-2997
2.493	199.9	-8.176	-1.805	-16.76	-47.84	-20.71	-172.4	-30.07	-474.4	-39.56	-988.9	-49.64	-1774	-64.02	-3081
.0001	150.0	-8.248	-2.472	-17.15	-53.33	-20.98	-182.8	-31.11	-508.5	-40	-1024	-50.71	-1853	-64.70	-3165
-1.869	112.6	-8.334	-3.253	-17.46	-58.92	-21.26	-193.7	-32.06	-542.4	-40.45	-1060	-51.83	-1937	-65.36	-3250
-3.319	83.47	-8.439	-4.157	-17.73	-64.67	-21.56	-205.1	-32.91	-575.5	-40.91	-1097	-53	-2025	-66.02	-3335
-4.471	60.54	-8.567	-5.193	-17.96	-70.60	-21.88	-217.2	-33.66	-607.8	-41.38	-1136	(7)		-66.68	-3422
-5.396	42.42	-8.726	-6.378	-18.18	-76.74	-22.23	-229.9	-34.33	-639.4	-41.87	-1175	-54.18	-2116	-67.37	-3510
-6.144	28.31	-8.925	-7.735	-18.38	-83.11	-22.61	-243.6	-34.93	-670.4	-42.38	-1216	-55.34	-2209	-68	-3600
-6.747	17.64	-9.181	-9.305	-18.58	-89.72	-23.03	-258.2								
Curve V															
(5)		-8.024	486.0	-18.08	-1.783	-21.03	-32.60	-32.17	-139.7	-34.72	-303.9	-40.71	-589.1	-53.43	-1130
+∞	+∞	-10.70	343.7	-18.12	-2.790	-22.55	-39.43	-32.38	-150.9	-34.98	-321.1	-41.93	-630.2	-53.96	-1172
1657	85340	-12.81	233.3	-18.18	-4.027	-25	-49	-32.58	-162.4	-35.26	-339.0	-43.38	-677.0	-54.46	-1217
407.1	21950	-14.47	148.4	-18.25	-5.497	(3)		-32.78	-174.4	-35.57	-357.6	-45	-729	-54.93	-1263
172.6	9925	-15.76	85.45	-18.34	-7.204	-27.56	-60.16	-32.97	-186.8	-35.90	-377.1	(5)		-55.39	-1309
89.30	5614	-16.73	42.35	-18.44	-9.158	-29.18	-70.51	-33.17	-199.7	-36.25	-397.6	-46.65	-784.0	-55.83	-1355
50.12	3568	-17.45	15.69	-18.57	-11.37	-30.11	-80.10	-33.37	-213.0	-36.65	-419.1	-48.17	-838.8	-56.26	-1402
28.44	2427	-18	0	-18.73	-13.85	-30.70	-89.48	-33.57	-226.8	-37.10	-441.9	-49.46	-891.5	-56.69	-1450
15.10	1720	(1)		-18.94	-16.64	-31.12	-98.94	-33.78	-241.2	-37.60	-466.3	-50.54	-941.6	-57.12	-1499
6.229	1248	-18.01	-.1111	-19.21	-19.77	-31.44	-108.6	-34	-256	-38.19	-492.5	-51.43	-989.6	-57.56	-1549
-.0002	915.1	-18.02	-.4447	-19.59	-23.34	-31.72	-118.6	-34.23	-271.4	-38.88	-521.3	-52.18	-1036	-58	-1600
-4.567	670.7	-18.04	-1.002	-20.14	-27.49	-31.95	-129.0	-34.46	-287.3	-39.70	-553.2	-52.84	-1082		

*Numbers in parentheses are the mode numbers m having (m - 1) lines of zero deflection.

TABLE 1.- SOLUTIONS OF FREQUENCY EQUATIONS IN TERMS OF $\bar{A}$ AND $\bar{B}$ FOR CLAMPED SUPPORTS WITH $q_x = \infty$ - Concluded

(b) Asymmetrical modes

$\bar{A}$	$\bar{B}$	$\bar{A}$	$\bar{B}$	$\bar{A}$	$\bar{B}$	$\bar{A}$	$\bar{B}$	$\bar{A}$	$\bar{B}$	$\bar{A}$	$\bar{B}$	$\bar{A}$	$\bar{B}$	$\bar{A}$	$\bar{B}$
Curve II															
(2)		-4.115	-0.2278	-5.524	-14.27	-12.14	-95.49	-18.80	-288.6	-28.87	-711.5	-39.30	-1400	-52.78	-2568
+∞	+∞	-4.133	-.4057	-5.684	-15.89	-12.59	-103.8	-19.20	-303.3	-29.55	-746.5	-39.92	-1448	-53.70	-2659
273.9	2332	-4.156	-.6354	-5.858	-17.67	-13.01	-112.1	-19.63	-318.9	-30.20	-781.7	-40.54	-1497	-54.60	-2750
69.44	638.9	-4.185	-.9176	-6.048	-19.61	-13.40	-120.4	-20.07	-335.4	-30.84	-816.9	-41.19	-1549	-55.48	-2841
30.34	306.9	-4.219	-1.253	-6.255	-21.75	-13.77	-128.8	-20.53	-353.0	-31.45	-852.1	-41.86	-1603	-56.34	-2933
16.15	183.9	-4.259	-1.643	-6.483	-24.11	-14.11	-137.4	-21.02	-371.7	-32.04	-887.4	-42.55	-1659	-57.18	-3024
9.336	123.8	-4.304	-2.089	-6.734	-26.73	-14.44	-146.1	-21.54	-391.7	-32.61	-922.9	-43.27	-1719	-58.00	-3116
5.444	88.92	-4.355	-2.593	-7.012	-29.66	-14.77	-154.9	-22.09	-413.1	-33.17	-958.6	-44.02	-1781	-58.80	-3207
2.966	66.42	-4.412	-3.156	-7.320	-32.95	-15.09	-164.0	-22.66	-436.0	-33.73	-994.8	-44.79	-1846	-59.60	-3299
1.252	50.67	-4.475	-3.780	-7.663	-36.66	-15.40	-173.4	-23.27	-460.6	-34.27	-1031	-45.60	-1914	-60.38	-3392
-.0104	38.93	-4.545	-4.469	-8.046	-40.88	-15.71	-183.0	-23.92	-486.9	-34.82	-1068	-46.43	-1985	-61.15	-3485
-.9779	29.88	-4.621	-5.225	-8.472	-45.65	-16.03	-192.9	-24.59	-515.0	-35.36	-1106	-47.29	-2060	-61.92	-3579
-1.763	22.45	-4.704	-6.051	-8.943	-51.08	-16.35	-203.2	-25.28	-544.7	-35.90	-1145	-48.17	-2139	-62.69	-3674
-2.412	16.26	-4.795	-6.593	-9.455	-57.20	-16.67	-213.9	-26	-576	-36.45	-1184	-49.08	-2220	-63.46	-3771
-2.968	10.92	-4.893	-7.934	-10	-64	-17	-225	(6)		-37	-1225	-50	-2304	-64.23	-3869
-3.457	6.193	-5	-9	(4)		-17.34	-236.6	-26.73	-608.6	-37.56	-1267	(8)		-65	-3969
-3.887	2.036	-5.116	-10.16	-10.56	-71.38	-17.69	-248.7	-27.45	-642.3	-38.13	-1310	-50.93	-2390		
-4.094	-.0253	-5.241	-11.42	-11.11	-79.20	-18.04	-261.3	-28.17	-676.7	-38.71	-1354	-51.86	-2479		
-4.102	-.1011	-5.377	-12.78	-11.64	-87.28	-18.42	-274.6								
Curve IV															
(4)		-10.91	36.07	-12.62	-14.90	-15.52	-78.52	-26.07	-286.9	-31.68	-595.8	-44.18	-1258	-54.13	-2146
+∞	+∞	-11.72	11.00	-12.70	-17.16	-15.97	-85.94	-26.42	-302.5	-32.15	-622.2	-45.06	-1314	-54.72	-2209
1066	35340	(2)		-12.80	-19.60	-16.51	-94.37	-26.76	-318.4	-32.66	-650.1	-45.86	-1370	-55.32	-2274
263.3	9188	-12.10	-.0747	-12.89	-22.21	-17.17	-104.1	-27.08	-334.6	-33.21	-679.9	-46.60	-1424	-55.94	-2341
112.2	4198	-12.11	-.2987	-13	-25	-17.97	-115.5	-27.40	-351.2	-33.81	-711.8	-47.29	-1478	-56.59	-2410
58.37	2399	-12.12	-.6724	-13.12	-27.99	-18.92	-128.8	-27.71	-368.2	-34.47	-746.1	-47.94	-1531	-57.27	-2483
32.93	1540	-12.14	-1.196	-13.24	-31.17	-20	-144	-28.03	-385.6	-35.20	-783.3	-48.55	-1584	-57.98	-2559
18.77	1058	-12.16	-1.870	-13.38	-34.57	(4)		-28.35	-403.5	-36.00	-823.8	-49.14	-1637	-58.73	-2638
9.998	756.2	-12.19	-2.696	-13.53	-38.18	-21.11	-160.5	-28.67	-422.0	-36.89	-868.1	-49.71	-1691	-59.53	-2722
4.151	554.2	-12.22	-3.674	-13.69	-42.04	-22.13	-177.4	-29	-441	-37.86	-916.3	-50.26	-1744	-60.37	-2810
-.0001	410.0	-12.26	-4.805	-13.87	-46.16	-23.00	-193.9	-29.34	-460.7	-38.90	-968.5	-50.81	-1799	-61.28	-2904
-3.071	303.2	-12.31	-6.090	-14.07	-50.56	-23.73	-210.0	-29.69	-480.9	-40	-1024	-51.36	-1854	-62.24	-3004
-5.420	221.6	-12.36	-7.532	-14.29	-55.28	-24.34	-225.6	-30.05	-502.1	(6)		-51.90	-1910	-63.27	-3110
-7.265	157.8	-12.41	-9.132	-14.54	-60.36	-24.85	-240.9	-30.43	-524.0	-41.11	-1082	-52.45	-1967	-64.37	-3223
-8.735	107.7	-12.48	-10.89	-14.82	-65.87	-25.30	-256.2	-30.82	-546.9	-42.20	-1141	-53	-2025	-65.53	-3343
-9.929	67.79	-12.55	-12.82	-15.14	-71.88	-25.70	-271.5	-31.24	-570.7	-43.23	-1200	-53.56	-2085	-66.75	-3469
														-68	-3600
Curve VI															
(6)		-11.14	936.6	-24.19	-5.363	-25	-49	-27.20	-134.4	-39.51	-365.8	-44.03	-642.5	-48.20	-1003
+∞	+∞	-14.82	658.4	-24.22	-7.303	-25.11	-54.72	-27.61	-145.7	-40.21	-390.3	-44.35	-670.6	-48.73	-1044
2377	175700	-17.68	443.9	-24.26	-9.546	-25.24	-60.80	-28.12	-158.0	-40.77	-414.3	-44.67	-699.4	-49.31	-1087
581.9	44860	-19.93	279.1	-24.31	-12.09	-25.38	-67.23	-28.76	-171.8	-41.25	-438.3	-45	-729	-49.97	-1133
245.8	20140	-21.70	154.2	-24.36	-14.94	-25.53	-74.04	-29.60	-187.7	-41.68	-462.3	-45.34	-759.4	-50.70	-1183
126.8	11320	-23.07	62.78	-24.41	-18.10	-25.69	-81.23	-30.72	-206.5	-42.06	-486.7	-45.69	-790.7	-51.55	-1236
70.92	7143	(2)		-24.48	-21.56	-25.87	-88.84	-34	-256	-42.41	-511.4	-46.05	-823.0	-52.52	-1295
40.11	4827	-24.10	-.1487	-24.55	-25.33	-26.08	-96.88	(4)		-42.75	-536.5	-46.43	-856.3	-53.65	-1361
21.22	3398	-24.11	-.5950	-24.62	-29.42	-26.30	-105.4	-35.85	-285.1	-43.08	-562.1	-46.83	-890.8	-54.95	-1433
8.724	2449	-24.12	-1.339	-24.70	-33.83	-26.56	-114.4	-37.42	-313.7	-43.40	-588.3	-47.25	-926.6	-56.42	-1513
-.0112	1784	-24.14	-2.381	-24.80	-38.56	-26.85	-124.1	-38.61	-340.5	-43.71	-615.1	-47.71	-963.9	-58	-1600
-6.358	1300	-24.16	-3.722	-24.89	-43.61										

TABLE 2.- SOLUTIONS OF FREQUENCY EQUATIONS IN TERMS OF $\bar{A}$ AND $\bar{B}$ FOR FINITE ROTATIONAL RESTRAINTS WITH $q_x = 40$

(a) Symmetrical modes

$\bar{A}$	$\bar{B}$	$\bar{A}$	$\bar{B}$	$\bar{A}$	$\bar{B}$	$\bar{A}$	$\bar{B}$	$\bar{A}$	$\bar{B}$	$\bar{A}$	$\bar{B}$	$\bar{A}$	$\bar{B}$	$\bar{A}$	$\bar{B}$
Curve I															
(1)		-1.820	-0.0112	(3)		-9.680	-63.95	(5)		-25.54	-569.7	(7)		-49.40	-2278
+∞	+∞	-1.834	-.0451	-5.532	-11.09	-9.918	-68.54	-17.62	-241.8	-26.00	-593.3	-37.81	-1279	-50.08	-2346
27.78	63.14	-1.857	-.1024	-5.987	-13.26	-10.17	-73.43	-18.20	-258.6	-26.48	-618.0	-38.58	-1333	-50.79	-2417
9.810	25.75	-1.890	-.1843	-6.357	-15.45	-10.43	-78.67	-18.75	-275.4	-26.98	-644.0	-39.33	-1387	-51.52	-2490
4.972	15.39	-1.934	-.2925	-6.660	-17.67	-10.72	-84.29	-19.26	-292.1	-27.50	-671.5	-40.03	-1440	-52.28	-2567
2.841	10.72	-1.990	-.4298	-6.917	-19.92	-11.02	-90.34	-19.74	-308.7	-28.04	-700.6	-40.72	-1492	-53.07	-2648
1.663	8.096	-2.058	-.5997	-7.142	-22.24	-11.34	-96.88	-20.19	-325.2	-28.62	-731.4	-41.37	-1544	-53.89	-2733
.9103	6.397	-2.142	-.8070	-7.348	-24.63	-11.69	-104.0	-20.62	-341.8	-29.22	-764.3	-42.01	-1596	-54.75	-2823
.3799	5.187	-2.242	-1.059	-7.540	-27.11	-12.07	-111.8	-21.04	-358.5	-29.86	-799.3	-42.63	-1648	-55.65	-2917
-.0223	4.260	-2.363	-1.364	-7.725	-29.70	-12.47	-120.3	-21.45	-375.4	-30.54	-836.8	-43.24	-1701	-56.59	-3017
-.3448	3.511	-2.510	-1.735	-7.906	-32.41	-12.92	-129.6	-21.85	-392.6	-31.25	-876.9	-43.84	-1753	-57.57	-3122
-.6153	2.878	-2.688	-2.192	-8.086	-35.24	-13.40	-140.0	-22.24	-410.0	-32.01	-919.8	-44.44	-1807	-58.59	-3233
-.8503	2.323	-2.907	-2.760	-8.267	-38.21	-13.92	-151.4	-22.64	-427.9	-32.80	-965.4	-45.03	-1861	-59.64	-3348
-1.061	1.824	-3.178	-3.480	-8.451	-41.33	-14.49	-164.0	-23.03	-446.2	-33.62	-1014	-45.63	-1916	-60.71	-3468
-1.253	1.365	-3.518	-4.404	-8.638	-44.61	-15.09	-177.8	-23.43	-465.1	-34.46	-1064	-46.23	-1972	-61.80	-3591
-1.433	.9307	-3.940	-5.602	-8.831	-48.07	-15.72	-192.7	-23.83	-484.5	-35.32	-1117	-46.84	-2030	-62.88	-3716
-1.604	.5179	-4.446	-7.136	-9.030	-51.71	-16.36	-208.5	-24.24	-504.6	-36.17	-1171	-47.46	-2089	-63.95	-3843
-1.768	.1172	-5	-9	-9.238	-55.56	-17	-225	-24.66	-525.4	-37	-1225	-48.09	-2150	-65	-3969
Curve III															
(3)		(1)		-11.48	-19.68	-17.80	-102.5	-23.59	-294.7	-34.82	-720.4	-42.74	-1321	-58.19	-2501
+∞	+∞	-7.280	-0.0449	-13	-25	-17.99	-109.6	-24.47	-318.1	-35.20	-747.9	-43.53	-1376	-58.83	-2574
114.7	2228	-7.294	-.1799	(3)		-18.12	-117.0	-25.51	-345.1	-35.57	-775.7	-44.41	-1436	-59.44	-2645
41.45	896.1	-7.316	-.4057	-14.21	-30.43	-18.38	-124.7	-26.67	-375.4	-35.95	-804.1	-45.40	-1503	-60.03	-2717
20.10	503.6	-7.348	-.7233	-14.98	-35.46	-18.80	-141.0	-27.86	-408.0	-36.33	-833.2	-46.52	-1577	-60.61	-2789
10.41	324.0	-7.391	-1.135	-15.48	-40.28	-19.03	-149.8	-29	-441	-36.71	-862.9	-47.75	-1659	-61.18	-2861
5.004	223.0	-7.445	-1.642	-15.83	-45.08	-19.27	-158.9	(5)		-37.10	-893.3	-49.07	-1747	-61.75	-2934
1.600	159.0	-7.512	-2.249	-16.11	-49.95	-19.53	-168.5	-30.00	-473.0	-37.49	-924.6	-50.43	-1840	-62.31	-3008
-.7588	114.5	-7.595	-2.961	-16.35	-54.96	-19.81	-178.6	-30.84	-503.3	-38.33	-990.3	-51.76	-1933	-62.88	-3084
-2.471	82.14	-7.697	-3.786	-16.55	-60.14	-20.11	-189.4	-31.55	-532.1	-38.77	-1025	-53	-2025	-63.45	-3160
-3.766	57.80	-7.823	-4.734	-16.74	-65.51	-20.44	-200.8	-32.15	-559.9	-39.23	-1061	(7)		-64.03	-3238
-4.771	39.20	-7.981	-5.821	-16.92	-71.09	-20.81	-213.0	-32.69	-586.9	-39.71	-1098	-54.11	-2113	-64,62	-3318
-5.557	25.12	-8.183	-7.077	-17.10	-76.90	-21.22	-226.2	-33.17	-613.6	-40.23	-1138	-55.11	-2197	-65.86	-3485
-6.172	14.81	-8.452	-8.545	-17.27	-82.93	-21.68	-240.6	-33.61	-640.1	-40.78	-1179	-55.99	-2277	-66.51	-3573
-6.656	7.531	-8.825	-10.31	-17.45	-89.21	-22.22	-256.5	-34.03	-666.7	-41.38	-1223	-56.79	-2354	-67.18	-3664
-7.049	2.490	-9.372	-12.53	-17.62	-95.74	-22.85	-274.4	-34.43	-693.4	-42.02	-1270	-57.51	-2428	-67.90	-3758
		-10.21	-15.51												
Curve V															
(5)		(1)		-17.54	-18.03	-29.52	-110.2	-32.10	-279.3	-41.02	-615.1	-51.58	-1144	-57.21	-1796
+∞	+∞	-16.42	-0.1014	-17.93	-21.33	-29.70	-119.6	-32.34	-295.0	-43.12	-672.5	-51.94	-1185	-57.77	-1855
34.11	2534	-16.44	-.4057	-18.54	-25.27	-29.87	-129.4	-32.61	-311.4	-45	-729	-52.30	-1226	-58.40	-1917
15.49	1589	-16.46	-.9136	-19.65	-30.43	-30.04	-139.5	-32.89	-328.5	(5)		-52.65	-1267	-59.11	-1984
5.016	1055	-16.49	-1.626	-21.85	-38.19	-30.20	-150.1	-33.21	-346.4	-46.44	-780.0	-53.01	-1309	-59.92	-2056
-1.610	717.5	-16.53	-2.545	-25	-49	-30.37	-161.0	-33.56	-365.3	-47.51	-826.0	-53.37	-1353	-60.86	-2136
-6.127	487.5	-16.58	-3.672	(3)		-30.54	-172.3	-33.96	-385.4	-48.32	-868.5	-53.74	-1397	-62.00	-2226
-9.359	323.8	-16.64	-5.011	-26.98	-58.88	-30.71	-184.1	-34.42	-406.9	-48.97	-909.1	-54.11	-1442	-63.37	-2329
-11.75	203.9	-16.72	-6.567	-27.93	-67.43	-30.88	-196.3	-34.97	-430.3	-49.51	-948.5	-54.90	-1535	-65.04	-2448
-13.53	117.1	-16.82	-8.346	-28.46	-75.63	-31.06	-208.9	-35.64	-456.4	-49.99	-987.4	-55.31	-1584	-67.01	-2585
-14.83	57.47	-16.94	-10.36	-28.82	-83.88	-31.25	-222.0	-36.50	-486.1	-50.42	-1026	-55.74	-1634	-69.15	-2734
-15.72	21.31	-17.09	-12.62	-29.09	-92.34	-31.65	-249.6	-37.63	-521.1	-50.83	-1065	-56.20	-1686	-71.21	-2884
-16.34	2.010	-17.28	-15.16	-29.32	-101.1	-31.87	-264.2	-39.12	-563.7	-51.21	-1105	-56.68	-1740	-73	-3025

TABLE 2.- SOLUTIONS OF FREQUENCY EQUATIONS IN TERMS OF $\bar{A}$ AND $\bar{B}$ FOR FINITE ROTATIONAL RESTRAINTS WITH $q_x = 40$ - Concluded

(b) Asymmetrical modes

$\bar{A}$	$\bar{B}$	$\bar{A}$	$\bar{B}$	$\bar{A}$	$\bar{B}$	$\bar{A}$	$\bar{B}$	$\bar{A}$	$\bar{B}$	$\bar{A}$	$\bar{B}$	$\bar{A}$	$\bar{B}$	$\bar{A}$	$\bar{B}$
							Curve II								
(2)		-3.773	-0.3702	-5.326	-14.73	-11.91	-93.26	-18.11	-273.6	-28.64	-703.3	-38.89	-1391	-52.63	-2557
+∞	+∞	-3.796	-.5798	-5.505	-16.41	-12.29	-100.6	-18.53	-288.3	-29.22	-734.5	-39.55	-1441	-53.44	-2639
69.28	603.3	-3.824	-.8375	-5.702	-18.28	-12.63	-107.9	-18.98	-304.0	-29.77	-765.6	-40.25	-1495	-54.22	-2720
24.89	241.7	-3.858	-1.144	-5.919	-20.35	-12.96	-115.4	-19.46	-320.9	-30.31	-796.6	-40.99	-1551	-54.98	-2801
12.32	137.7	-3.897	-1.500	-6.160	-22.66	-13.27	-122.9	-19.96	-339.1	-30.83	-827.8	-41.76	-1611	-55.71	-2882
6.689	90.45	-3.942	-1.908	-6.428	-25.25	-13.57	-130.6	-20.51	-358.7	-31.34	-859.1	-42.57	-1675	-56.43	-2962
3.566	63.92	-3.992	-2.369	-6.729	-28.19	-13.87	-138.5	-21.09	-379.9	-31.84	-890.8	-43.41	-1742	-57.14	-3043
1.589	46.94	-4.048	-2.884	-7.067	-31.55	-14.16	-146.5	-21.71	-402.9	-32.34	-923.0	-44.30	-1814	-57.84	-3125
.2185	35.06	-4.111	-3.457	-7.449	-35.39	-14.45	-154.9	-22.37	-427.8	-32.83	-955.8	-45.22	-1889	-58.54	-3207
-.7998	26.15	-4.180	-4.088	-7.878	-39.81	-14.74	-163.5	-23.06	-454.5	-33.33	-989.2	-46.17	-1968	-59.24	-3290
-1.589	19.20	-4.255	-4.783	-8.358	-44.89	-15.03	-172.4	-23.78	-483.0	-33.83	-1023	-47.13	-2050	-59.93	-3375
-2.233	13.48	-4.338	-5.543	-8.883	-50.66	-15.33	-181.7	-24.52	-513.0	-34.34	-1059	-48.10	-2134	-60.64	-3461
-2.777	8.619	-4.428	-6.374	-9.438	-57.08	-15.64	-191.3	-25.27	-544.2	-34.85	-1095	-49.06	-2219	-61.35	-3549
-3.246	4.398	-4.527	-7.280	-10	-64	-15.95	-201.4	-26	-576	-35.38	-1132	-50	-2304	-62.07	-3639
-3.643	.9155	-4.750	-9.343	(4)		-16.61	-223.0	(6)		-36.47	-1211	(8)		-62.81	-3732
-3.735	-.0230	-4.876	-10.52	-10.54	-71.23	-16.96	-234.6	-26.71	-608.1	-37.04	-1253	-50.91	-2389	-64.33	-3927
-3.742	-.0923	-5.013	-11.79	-11.04	-78.57	-17.32	-246.9	-27.39	-640.1	-37.63	-1297	-51.79	-2473	-65.13	-4030
-3.755	-.2078	-5.163	-13.19	-11.50	-85.93	-17.71	-259.9	-28.03	-671.8	-38.25	-1342				
							Curve IV								
(4)		-11.07	-0.2731	-12.04	-25.59	-17.62	-113.0	-25.50	-312.1	-31.61	-639.3	-44.67	-1325	-52.81	-2136
+∞	+∞	-11.08	-.6147	-12.16	-28.50	-18.82	-128.0	-25.78	-327.1	-32.32	-672.9	-45.21	-1371	-53.44	-2201
161.4	5580	-11.10	-1.093	-12.29	-31.61	-20	-144	-26.06	-342.6	-33.14	-710.2	-45.72	-1416	-54.12	-2269
58.09	2249	-11.12	-1.710	-12.44	-34.94	(4)		-26.34	-358.5	-34.07	-752.1	-46.22	-1462	-54.84	-2342
27.49	1256	-11.15	-2.465	-12.60	-38.48	-21.01	-159.7	-26.63	-374.9	-35.14	-799.2	-46.71	-1508	-55.63	-2419
13.45	797.5	-11.18	-3.358	-12.78	-42.28	-21.80	-174.4	-26.93	-391.8	-36.32	-851.5	-47.18	-1554	-56.49	-2503
5.569	538.7	-11.22	-4.392	-12.98	-46.35	-22.42	-188.5	-27.56	-427.5	-37.58	-907.8	-47.65	-1601	-57.44	-2593
.5813	374.4	-11.26	-5.567	-13.20	-50.74	-22.92	-202.0	-27.90	-446.4	-38.83	-966.2	-48.13	-1649	-58.49	-2692
-2.832	261.9	-11.31	-6.885	-13.46	-55.50	-23.34	-215.3	-28.25	-466.0	-40	-1024	-48.60	-1698	-59.66	-2801
-5.298	180.9	-11.36	-8.348	-13.76	-60.72	-23.71	-228.6	-28.62	-486.6	(6)		-49.08	-1747	-60.94	-2919
-7.149	120.5	-11.42	-9.957	-14.11	-66.50	-24.05	-241.9	-29.02	-508.1	-41.04	-1080	-49.56	-1798	-62.33	-3047
-8.573	74.86	-11.49	-11.71	-14.53	-73.03	-24.36	-255.4	-29.45	-530.9	-41.95	-1132	-50.06	-1850	-63.79	-3183
-9.689	40.05	-11.56	-13.62	-15.06	-80.54	-24.66	-269.1	-29.91	-555.1	-42.75	-1183	-51.09	-1958	-65.26	-3324
-10.58	13.59	-11.64	-15.69	-15.72	-89.41	-24.94	-283.1	-30.42	-581.0	-43.45	-1231	-51.64	-2015	-66.68	-3464
(2)		-11.73	-17.91	-16.57	-100.1	-25.22	-297.4	-30.98	-608.9	-44.08	-1279	-52.21	-2075	-68	-3600
-11.06	-.0683	-11.82	-20.30												
							Curve VI								
(6)		-19.78	146.5	-22.29	-11.08	-23.28	-61.51	-26.81	-159.5	-38.61	-390.8	-41.40	-621.3	-45.53	-965.4
+∞	+∞	-21.33	46.16	-22.34	-13.69	-23.42	-67.73	-27.95	-176.6	-38.94	-411.8	-41.68	-647.5	-46.17	-1007
255.4	20070	(2)		-22.39	-16.58	-23.57	-74.29	-29.62	-198.7	-39.24	-433.2	-42.27	-702.2	-46.92	-1054
86.95	8091	-22.10	-.1364	-22.45	-19.76	-23.74	-81.23	-31.84	-226.5	-39.52	-454.9	-42.59	-730.7	-47.82	-1105
39.57	4456	-22.11	-.5457	-22.51	-23.21	-23.92	-88.58	-34	-256	-39.79	-477.1	-42.92	-760.2	-48.95	-1164
16.33	2764	-22.12	-1.228	-22.58	-26.96	-24.14	-96.37	(4)		-40.06	-499.7	-43.27	-790.7	-50.37	-1234
3.208	1806	-22.13	-2.184	-22.66	-30.99	-24.38	-104.7	-35.56	-282.6	-40.32	-522.9	-43.64	-822.4	-52.12	-1316
-5.094	1200	-22.16	-3.413	-22.74	-35.31	-24.67	-113.5	-36.58	-306.2	-40.59	-546.6	-44.05	-855.4	-54.15	-1409
-10.73	790.0	-22.18	-4.917	-22.83	-39.93	-25.02	-123.2	-37.29	-328.0	-40.85	-570.9	-44.49	-890.0	-56.21	-1507
-14.74	500.6	-22.21	-6.696	-23.04	-50.09	-25.46	-133.7	-37.82	-349.1	-41.12	-595.8	-44.98	-926.5	-58	-1600
-17.66	293.1	-22.25	-8.751	-23.15	-55.64	-26.03	-145.6	-38.24	-369.9						

TABLE 3.- SOLUTIONS OF FREQUENCY EQUATIONS IN TERMS OF $\bar{A}$ AND $\bar{B}$ FOR FINITE ROTATIONAL RESTRAINTS WITH $q_x = 10$

(a) Symmetrical modes

$\bar{A}$	$\bar{B}$	$\bar{A}$	$\bar{B}$	$\bar{A}$	$\bar{B}$	$\bar{A}$	$\bar{B}$	$\bar{A}$	$\bar{B}$	$\bar{A}$	$\bar{B}$	$\bar{A}$	$\bar{B}$	$\bar{A}$	$\bar{B}$
Curve I															
(1)		-1.533	-0.2306	-6.214	-16.33	-9.553	-72.21	-18.84	-283.4	-25.09	-576.9	-38.42	-1325	-47.62	-2162
$+\infty$	$+\infty$	-1.582	-.3393	-6.381	-18.17	-9.836	-77.46	-19.19	-296.9	-25.57	-601.1	-39.02	-1370	-48.24	-2223
10.57	24.81	-1.644	-.4744	-6.533	-20.07	-10.15	-83.23	-19.52	-310.2	-26.09	-627.1	-39.56	-1414	-48.90	-2287
3.975	11.34	-1.720	-.6404	-6.678	-22.04	-10.49	-89.62	-19.83	-323.6	-26.64	-655.4	-40.08	-1457	-49.59	-2356
1.935	7.119	-1.812	-.8435	-6.819	-24.10	-10.87	-96.79	-20.14	-337.2	-27.25	-686.4	-40.57	-1499	-50.34	-2429
.9429	5.049	-1.925	-1.093	-6.960	-26.26	-11.30	-104.9	-20.45	-351.0	-27.92	-720.7	-41.05	-1541	-51.14	-2509
.3440	3.789	-2.064	-1.402	-7.102	-28.51	-11.79	-114.3	-20.76	-365.0	-28.67	-759.1	-41.52	-1583	-52.02	-2596
-.0680	2.919	-2.239	-1.793	-7.245	-30.88	-12.35	-125.1	-21.07	-379.4	-29.50	-802.5	-41.99	-1625	-52.97	-2691
-.3803	2.254	-2.463	-2.298	-7.394	-33.36	-13.01	-137.9	-21.38	-394.2	-30.45	-851.8	-42.45	-1668	-54.03	-2797
-.6320	1.716	-2.759	-2.972	-7.546	-35.97	-13.77	-152.9	-21.70	-409.3	-31.50	-907.8	-42.92	-1711	-55.21	-2916
-.8454	1.258	-3.158	-3.904	-7.704	-38.71	-14.62	-170.2	-22.03	-425.0	-32.67	-970.4	-43.40	-1756	-56.53	-3050
-1.033	.8543	-3.699	-5.221	-7.869	-41.60	-15.49	-188.9	-22.36	-441.2	-33.88	-1037	-43.88	-1801	-57.98	-3198
-1.205	.4829	-4.366	-6.993	-8.041	-44.65	-16.31	-207.6	-22.70	-458.0	-35.06	-1105	-44.37	-1848	-59.54	-3360
-1.364	.1366	-5	-9	-8.221	-47.87	-17	-225	-23.06	-475.5	-36.11	-1168	-44.87	-1895	-61.11	-3527
-1.431	-.0088	(3)		-8.611	-54.91	(5)		-23.81	-512.9	-37	-1225	-45.38	-1945	-62.59	-3688
-1.443	-.0355	-5.464	-10.94	-8.823	-58.78	-17.57	-241.0	-24.22	-533.0	(7)		-45.91	-1996	-63.89	-3836
-1.464	-.0806	-5.785	-12.76	-9.049	-62.93	-18.05	-255.8	-24.64	-554.3	-37.77	-1277	-47.02	-2104	-65	-3919
-1.494	-.1451	-6.022	-14.54	-9.292	-67.38	-18.47	-269.8								
Curve III															
(3)		-6.146	-1.353	-14.47	-37.54	-16.82	-130.0	-29	-441	-34.15	-787.7	-43.50	-1465	-58.66	-2702
$+\infty$	$+\infty$	-6.192	-1.850	-14.64	-41.51	-17.00	-137.5	(5)		-34.43	-812.7	-45.94	-1601	-59.06	-2762
32.58	695.5	-6.249	-2.430	-14.78	-45.61	-17.18	-145.3	-29.83	-469.8	-34.72	-838.4	-48.96	-1769	-59.46	-2822
9.793	283.3	-6.318	-3.096	-14.91	-49.86	-17.38	-153.5	-30.37	-494.2	-35.33	-891.5	-51.47	-1919	-59.87	-2883
2.579	152.3	-6.402	-3.857	-15.04	-54.29	-17.60	-162.0	-30.78	-516.8	-35.64	-919.2	-53	-2025	-60.28	-2945
-.9337	88.41	-6.508	-4.722	-15.16	-58.89	-17.83	-171.0	-31.13	-538.6	-35.97	-947.7	(7)		-60.71	-3008
-3.009	50.78	-6.646	-5.710	-15.28	-63.68	-18.09	-180.5	-31.44	-560.1	-36.32	-977.1	-53.97	-2105	-61.13	-3072
-4.353	26.72	-6.834	-6.857	-15.40	-68.65	-18.38	-190.7	-31.73	-581.6	-36.68	-1008	-54.67	-2174	-62.02	-3204
-5.242	11.49	-7.112	-8.238	-15.52	-73.82	-18.72	-201.8	-32.00	-603.2	-37.07	-1039	-55.24	-2237	-62.48	-3272
-5.817	2.728	-7.579	-10.04	-15.64	-79.19	-19.12	-214.2	-32.27	-625.0	-37.48	-1073	-55.74	-2297	-62.96	-3343
(1)		-8.514	-12.83	-15.77	-84.77	-19.63	-228.5	-32.54	-647.1	-37.94	-1109	-56.20	-2355	-63.46	-3415
-6.032	-.0372	-10.62	-18.16	-15.91	-90.55	-20.30	-246.0	-32.80	-669.5	-38.45	-1147	-56.63	-2413	-63.98	-3490
-6.041	-.1490	-13	-25	-16.04	-96.55	-21.29	-269.0	-33.06	-692.3	-39.03	-1189	-57.05	-2470	-64.54	-3569
-6.057	-.3357	(3)		-16.19	-102.8	-22.81	-301.8	-33.33	-715.4	-39.74	-1238	-57.46	-2528	-65.13	-3651
-6.079	-.5980	-13.87	-29.67	-16.33	-109.2	-25.09	-349.2	-33.60	-739.0	-40.62	-1295	-57.86	-2585	-65.78	-3739
-6.109	-.9368	-14.24	-33.64	-16.65	-122.8	-27.51	-401.8	-33.87	-763.1	-41.81	-1367	-58.26	-2644	-66.51	-3835
														-67.35	-3942
Curve V															
(5)		-14.33	-2.206	-25	-49	-27.76	-146.5	-29.64	-305.7	(5)		-49.30	-1145	-52.90	-1667
$+\infty$	$+\infty$	-14.36	-3.179	(3)		-27.87	-156.5	-29.84	-320.9	-46.06	-773.0	-49.55	-1181	-53.25	-1714
48.75	3145	-14.40	-4.332	-26.19	-57.12	-27.99	-166.9	-30.05	-336.6	-46.61	-808.6	-49.79	-1218	-53.63	-1762
9.359	1171	-14.44	-5.665	-26.53	-63.99	-28.11	-177.7	-30.30	-353.1	-46.99	-841.9	-50.04	-1255	-54.05	-1813
-3.182	542.7	-14.49	-7.182	-26.73	-70.90	-28.24	-188.8	-30.57	-370.4	-47.30	-874.5	-50.30	-1293	-54.52	-1866
-9.182	242.9	-14.55	-8.886	-26.87	-78.05	-28.37	-200.2	-30.90	-388.9	-47.58	-907.0	-50.56	-1331	-55.09	-1925
-12.50	79.41	-14.62	-10.78	-26.99	-85.47	-28.65	-224.2	-31.33	-409.4	-47.84	-939.7	-51.10	-1410	-55.83	-1993
-14.13	5.084	-14.72	-12.88	-27.10	-93.21	-28.80	-236.8	-31.95	-433.5	-48.09	-972.7	-51.37	-1451	-56.95	-2079
(1)		-14.84	-15.21	-27.21	-101.3	-28.95	-249.8	-33.06	-466.3	-48.34	-1006	-51.66	-1492	-59.03	-2212
-14.27	-.0881	-15.01	-17.79	-27.32	-109.6	-29.11	-263.1	-35.67	-525.8	-48.58	-1040	-51.95	-1534	-63.64	-2471
-14.28	-.3524	-15.29	-20.75	-27.42	-118.3	-29.27	-276.8	-41.55	-645.2	-48.82	-1074	-52.25	-1576	-70.16	-2833
-14.29	-.7932	-15.91	-24.52	-27.53	-127.4	-29.45	-291.0	-45	-729	-49.06	-1109	-52.57	-1622	-73	-3025
-14.31	-1.411	-18.34	-31.92	-27.64	-136.8										

TABLE 3.- SOLUTIONS OF FREQUENCY EQUATIONS IN TERMS OF $\bar{A}$ AND $\bar{B}$ FOR FINITE ROTATIONAL RESTRAINTS WITH $q_x = 10$ - Concluded

(b) Asymmetrical modes

$\bar{A}$	$\bar{B}$	$\bar{A}$	$\bar{B}$	$\bar{A}$	$\bar{B}$	$\bar{A}$	$\bar{B}$	$\bar{A}$	$\bar{B}$	$\bar{A}$	$\bar{B}$	$\bar{A}$	$\bar{B}$	$\bar{A}$	$\bar{B}$
Curve II															
(2)		-3.285	-1.580	-5.613	-21.31	-12.69	-119.6	-19.65	-342.3	-30.22	-813.7	-39.45	-1471	-54.66	-2796
+∞	+∞	-3.330	-1.960	-5.928	-24.04	-12.92	-126.1	-20.40	-367.8	-30.60	-839.5	-40.35	-1538	-55.21	-2861
22.12	204.8	-3.381	-2.386	-6.302	-27.29	-13.38	-139.7	-21.26	-397.2	-30.99	-865.9	-41.36	-1613	-55.76	-2927
7.566	87.30	-3.437	-2.858	-6.749	-31.24	-13.62	-146.9	-22.22	-430.7	-31.39	-892.8	-42.49	-1698	-56.30	-2993
2.980	50.01	-3.500	-3.379	-7.290	-36.09	-13.86	-154.4	-23.26	-467.6	-31.79	-920.4	-43.74	-1793	-56.85	-3059
.7428	31.72	-3.568	-3.951	-7.934	-42.04	-14.11	-162.1	-24.28	-505.8	-32.19	-948.7	-45.11	-1897	-57.41	-3127
-.6024	20.67	-3.642	-4.577	-8.659	-49.06	-14.37	-170.2	-25.21	-542.4	-32.61	-978.0	-46.50	-2007	-57.97	-3197
-1.519	13.10	-3.724	-5.260	-9.379	-56.63	-14.64	-178.7	-26	-576	-33.04	-1008	-47.82	-2114	-58.54	-3268
-2.201	7.451	-3.813	-6.006	-10	-64	-15.21	-196.9	(6)		-33.48	-1039	-49.00	-2214	-59.12	-3341
-2.739	2.977	-4.014	-7.704	(4)		-15.52	-206.8	-26.67	-606.6	-34.42	-1106	-50	-2304	-59.72	-3416
-3.098	-.01911	-4.129	-8.671	-10.49	-70.83	-15.84	-217.2	-27.23	-634.9	-34.91	-1142	(8)		-60.33	-3494
-3.105	-.0765	-4.254	-9.729	-10.89	-77.20	-16.19	-228.4	-27.74	-661.7	-35.44	-1180	-50.86	-2385	-61.62	-3658
-3.116	-.1724	-4.392	-10.89	-11.22	-83.28	-16.56	-240.5	-28.20	-687.5	-35.99	-1220	-51.62	-2461	-62.32	-3745
-3.132	-.3069	-4.543	-12.17	-11.50	-89.23	-16.96	-253.5	-28.63	-712.9	-36.58	-1262	-52.30	-2531	-63.04	-3837
-3.153	-.4807	-4.710	-13.59	-11.76	-95.14	-17.39	-267.7	-29.04	-737.9	-37.21	-1308	-52.93	-2600	-63.80	-3935
-3.179	-.6941	-4.896	-15.17	-12.01	-101.1	-17.87	-283.3	-29.44	-763.0	-37.89	-1357	-53.53	-2666	-64.60	-4038
-3.209	-.9478	-5.104	-16.95	-12.24	-107.1	-18.39	-300.6	-29.83	-788.2	-38.63	-1412	-54.10	-2731	-65.46	-4149
-3.244	-1.243	-5.341	-18.97	-12.47	-113.3	-18.98	-320.1								
Curve IV															
(4)		-9.651	-2.896	-10.74	-32.41	(4)		-24.09	-322.3	-30.06	-640.9	-43.86	-1343	-49.33	-1972
+∞	+∞	-9.682	-3.786	-10.87	-35.49	-20.80	-157.9	-24.30	-336.0	-31.39	-692.4	-44.19	-1380	-49.80	-2024
41.47	1635	-9.717	-4.796	-11.01	-38.76	-21.26	-169.7	-24.52	-350.0	-33.39	-765.4	-44.52	-1417	-50.31	-2079
10.43	638.3	-9.756	-5.927	-11.17	-42.26	-21.59	-180.7	-24.98	-379.3	-36.08	-862.5	-44.86	-1455	-50.86	-2137
.5524	320.6	-9.800	-7.180	-11.35	-46.01	-21.86	-191.5	-25.23	-394.7	-38.52	-956.5	-45.19	-1494	-51.48	-2199
-4.234	166.8	-9.848	-8.556	-11.56	-50.09	-22.09	-202.3	-25.48	-410.5	-40	-1024	-45.53	-1533	-52.19	-2269
-7.005	78.50	-9.901	-10.06	-11.81	-54.59	-22.30	-213.2	-25.75	-426.9	(6)		-45.87	-1573	-53.04	-2349
-8.745	24.17	-9.958	-11.68	-12.13	-59.68	-22.50	-224.3	-26.03	-443.9	-40.89	-1075	-46.21	-1614	-54.12	-2445
(2)		-10.02	-13.43	-12.56	-65.71	-22.70	-235.6	-26.33	-461.7	-41.51	-1118	-46.57	-1655	-55.57	-2567
-9.553	-.05896	-10.09	-15.32	-13.19	-73.37	-22.89	-247.1	-26.66	-480.4	-42.00	-1157	-46.93	-1697	-57.61	-2732
-9.560	-.2359	-10.16	-17.33	-14.20	-84.16	-23.09	-258.9	-27.01	-500.2	-42.43	-1195	-47.67	-1784	-60.46	-2957
-9.570	-.5309	-10.33	-21.77	-15.94	-101.0	-23.28	-271.0	-27.41	-521.6	-42.81	-1232	-48.06	-1829	-63.79	-3222
-9.584	-.9441	-10.42	-24.20	-18.35	-124.4	-23.48	-283.3	-27.87	-545.0	-43.17	-1269	-48.47	-1875	-66.40	-3444
-9.602	-1.476	-10.52	-26.78	-20	-144	-23.68	-296.0	-28.42	-571.3	-43.52	-1306	-48.89	-1923	-68	-3600
-9.624	-2.126	-10.62	-29.51			-23.88	-309.0	-29.12	-602.3						
Curve VI															
(6)		-19.77	-1.098	-20.07	-20.67	-20.90	-71.15	-24.69	-163.5	-36.64	-385.6	-38.46	-591.7	-41.17	-881.1
+∞	+∞	-19.79	-1.952	-20.12	-23.98	-21.01	-77.34	-29.53	-209.0	-36.81	-404.2	-38.87	-638.6	-41.54	-913.5
54.33	5329	-19.80	-3.050	-20.18	-27.54	-21.13	-83.84	-34	-256	-36.99	-423.3	-39.08	-662.8	-42.00	-948.5
6.550	1884	-19.82	-4.393	-20.34	-31.36	-21.27	-90.65	(4)		-37.16	-442.8	-39.30	-687.6	-42.58	-988.0
-8.628	789.9	-19.85	-5.980	-20.30	-35.42	-21.42	-97.82	-35.07	-278.5	-37.34	-462.7	-39.53	-713.0	-43.45	-1036
-15.77	277.7	-19.87	-7.812	-20.45	-44.32	-21.60	-105.4	-35.53	-296.9	-37.52	-483.0	-39.76	-739.0	-45.03	-1107
-19.43	21.99	-19.91	-9.890	-20.52	-49.15	-21.81	-113.4	-35.83	-314.4	-37.70	-503.8	-40.01	-765.6	-48.68	-1244
(2)		-19.94	-12.21	-20.61	-54.25	-22.08	-122.2	-36.06	-331.8	-37.88	-525.1	-40.27	-793.0	-54.98	-1469
-19.76	-.1219	-19.98	-14.78	-20.70	-59.61	-22.47	-132.0	-36.27	-349.4	-38.07	-546.8	-40.54	-821.3	-58	-1600
-19.76	-.4878	-20.02	-17.60	-20.80	-65.24	-23.14	-144.2	-36.46	-367.3	-38.26	-569.0	-40.84	-850.6		

TABLE 4.- SOLUTIONS OF FREQUENCY EQUATIONS IN TERMS OF $\bar{A}$ AND $\bar{B}$ FOR FINITE ROTATIONAL RESTRAINTS WITH $q_x = 2$

(a) Symmetrical modes

$\bar{A}$	$\bar{B}$	$\bar{A}$	$\bar{B}$	$\bar{A}$	$\bar{B}$	$\bar{A}$	$\bar{B}$	$\bar{A}$	$\bar{B}$	$\bar{A}$	$\bar{B}$	$\bar{A}$	$\bar{B}$	$\bar{A}$	$\bar{B}$
Curve I															
(1)		-5.615	-14.54	-7.414	-46.23	-15.64	-196.0	-20.18	-367.3	-25.44	-629.7	-39.78	-1467	-45.97	-2070
+∞	+∞	-5.704	-15.96	-7.571	-49.05	-17	-225	-20.42	-379.3	-26.06	-660.8	-40.12	-1500	-46.46	-2118
2.007	5.713	-5.793	-17.44	-7.737	-52.03	(5)		-20.67	-391.6	-26.82	-699.0	-40.47	-1533	-46.98	-2169
.3418	2.368	-5.883	-18.97	-7.912	-55.18	-17.44	-238.4	-20.93	-404.2	-27.83	-749.5	-40.81	-1567	-47.54	-2224
-.2423	1.193	-5.976	-20.59	-8.099	-58.54	-17.72	-249.3	-21.19	-417.2	-29.30	-823.0	-41.16	-1601	-48.14	-2282
-.5661	.5403	-6.073	-22.26	-8.299	-62.16	-17.96	-259.6	-21.73	-444.3	-31.74	-946.0	-41.52	-1635	-48.79	-2347
-.7878	.0933	-6.172	-24.01	-8.516	-66.07	-18.18	-269.7	-22.01	-458.5	-35.41	-1134	-41.88	-1670	-49.55	-2421
-1.903	-2.161	-6.275	-25.84	-8.754	-70.37	-18.40	-279.8	-22.31	-473.2	-37	-1225	-42.25	-1706	-50.43	-2507
-2.395	-3.160	-6.383	-27.74	-9.020	-75.16	-18.61	-290.1	-22.62	-488.6	(7)		-42.62	-1743	-51.51	-2613
-3.553	-5.542	-6.494	-29.72	-9.327	-80.70	-18.83	-300.5	-22.94	-504.7	-37.61	-1269	-43.00	-1780	-52.93	-2753
-5	-9	-6.610	-31.79	-9.688	-87.22	-19.04	-311.1	-23.28	-521.7	-38.04	-1305	-43.39	-1818	-54.99	-2955
(3)		-6.730	-33.94	-10.14	-95.31	-19.26	-321.9	-23.64	-539.7	-38.41	-1338	-44.20	-1897	-58.40	-3291
-5.292	-10.55	-6.855	-36.19	-10.73	-106.0	-19.49	-332.9	-24.03	-559.0	-38.76	-1370	-44.62	-1938	-63.11	-3761
-5.424	-11.87	-6.986	-38.53	-11.60	-121.8	-19.71	-344.1	-24.45	-580.0	-39.10	-1403	-45.05	-1980	-65	-3969
-5.524	-13.19	-7.265	-43.54	-13.08	-148.6	-19.95	-355.6	-24.91	-603.1	-39.44	-1435	-45.50	-2024		
Curve III															
(3)		-13.79	-45.88	-15.47	-128.4	-29	-441	-31.97	-693.8	-35.64	-1049	-54.97	-2286	-59.92	-3081
+∞	+∞	-13.87	-49.81	-15.61	-135.0	(5)		-32.18	-714.9	-35.96	-1076	-55.28	-2336	-60.28	-3138
0.7368	100.9	-13.96	-53.90	-15.75	-141.8	-29.49	-463.5	-32.40	-736.4	-36.24	-1104	-55.59	-2385	-60.64	-3196
-4.351	9.465	-14.05	-58.14	-15.89	-148.8	-29.73	-481.8	-32.63	-758.2	-36.56	-1133	-55.90	-2436	-61.01	-3255
(1)		-14.14	-62.55	-16.04	-156.0	-29.94	-499.9	-32.86	-780.3	-36.93	-1165	-56.22	-2486	-61.38	-3315
-5.372	-6.979	-14.23	-67.13	-16.19	-163.3	-30.14	-518.0	-33.32	-825.7	-37.39	-1201	-56.54	-2538	-61.76	-3375
-5.518	-8.095	-14.32	-71.87	-16.35	-170.9	-30.33	-536.3	-33.56	-848.8	-38.25	-1257	-56.86	-2589	-62.14	-3437
-6.061	-10.02	-14.42	-76.76	-16.52	-178.8	-30.53	-554.9	-33.81	-872.4	-43.04	-1507	-57.19	-2642	-62.53	-3499
-13	-25	-14.53	-81.84	-16.70	-186.9	-30.73	-573.8	-34.05	-896.3	-53	-2025	-57.52	-2695	-62.93	-3562
(3)		-14.63	-87.07	-16.89	-195.4	-30.92	-593.0	-34.30	-920.6	(7)		-57.85	-2748	-63.35	-3627
-13.38	-28.57	-14.74	-92.47	-17.10	-204.4	-31.13	-612.6	-34.56	-945.3	-53.63	-2088	-58.18	-2802	-63.78	-3694
-13.48	-31.76	-14.86	-98.03	-17.38	-214.6	-31.33	-632.4	-34.82	-970.4	-54.01	-2139	-58.52	-2856	-64.24	-3764
-13.56	-35.06	-15.09	-109.7	-17.87	-228.7	-31.54	-652.5	-35.09	-996.0	-54.34	-2188	-58.87	-2912	-64.75	-3838
-13.64	-38.51	-15.21	-115.8	-20.41	-278.8	-31.75	-673.0	-35.36	-1022	-54.65	-2237	-59.56	-3024	-65.40	-3928
-13.71	-42.12	-15.34	-122.0												
Curve V															
(5)		-25.50	-61.44	-26.31	-138.4	-27.55	-259.0	-29.08	-402.5	-46.50	-909.9	-48.55	-1240	-51.19	-1663
+∞	+∞	-25.57	-67.76	-26.41	-147.8	-27.68	-271.8	-29.31	-419.6	-46.69	-940.6	-48.78	-1276	-51.45	-1705
-8.134	237.5	-25.64	-74.39	-26.51	-157.6	-27.82	-284.9	-29.80	-441.6	-46.89	-971.8	-49.23	-1349	-51.71	-1747
(1)		-25.72	-81.31	-26.61	-167.6	-27.95	-298.4	-45	-729	-47.08	-1004	-49.46	-1386	-51.99	-1790
-13.29	-17.98	-25.79	-88,55	-26.72	-177.9	-28.10	-312.2	(5)		-47.29	-1036	-49.70	-1424	-52.27	-1834
-13.37	-20.50	-25.87	-96.10	-26.82	-188.5	-28.25	-326.3	-45.51	-762.7	-47.49	-1068	-49.94	-1463	-52.56	-1879
-13.51	-23.31	-25.95	-103.9	-27.05	-210.8	-28.40	-340.8	-45.74	-791.7	-47.70	-1102	-50.18	-1502	-52.88	-1925
-25	-49	-26.04	-112.1	-27.17	-222.3	-28.56	-355.6	-45.93	-820.6	-47.90	-1135	-50.42	-1541	-53.26	-1975
(3)		-26.13	-120.6	-27.29	-234.2	-28.72	-370.8	-46.12	-849.9	-48.12	-1170	-50.67	-1581	-54.13	-2049
-25.41	-55.39	-26.22	-129.4	-27.42	-246.4	-28.89	-386.4	-46.31	-879.6	-48.33	-1205	-50.93	-1622	-73	-3025

TABLE 4.- SOLUTIONS OF FREQUENCY EQUATIONS IN TERMS OF $\bar{A}$ AND $\bar{B}$ FOR FINITE ROTATIONAL RESTRAINTS WITH $q_x = 2$ - Concluded

(b) Asymmetrical modes

$\bar{A}$	$\bar{B}$	$\bar{A}$	$\bar{B}$	$\bar{A}$	$\bar{B}$	$\bar{A}$	$\bar{B}$	$\bar{A}$	$\bar{B}$	$\bar{A}$	$\bar{B}$	$\bar{A}$	$\bar{B}$	$\bar{A}$	$\bar{B}$
Curve II															
(2)		-2.714	-2.917	-5.180	-22.75	-12.16	-122.4	-16.87	-273.0	-29.15	-779.2	-35.85	-1260	-53.66	-2732
+∞	+∞	-2.769	-3.364	-5.752	-27.38	-12.34	-127.9	-17.48	-292.4	-29.44	-799.8	-36.49	-1307	-54.07	-2784
2.307	37.45	-2.829	-3.847	-6.740	-35.37	-12.52	-133.6	-18.28	-318.1	-29.73	-820.7	-37.24	-1361	-54.48	-2835
-1.126	9.825	-2.894	-4.367	-8.680	-51.34	-12.70	-139.5	-19.45	-355.6	-30.03	-842.1	-38.17	-1427	-54.89	-2887
-2.352	-.0145	-3.039	-5.530	-10	-64	-12.89	-145.5	-21.41	-418.9	-30.34	-863.9	-39.38	-1515	-55.31	-2941
-2.358	-.0581	-3.120	-6.179	(4)		-13.08	-151.7	-24.54	-521.5	-30.65	-886.1	-41.14	-1642	-55.73	-2995
-2.367	-.1307	-3.206	-6.876	-10.36	-69.65	-13.50	-164.8	-26	-576	-30.96	-908.8	-44.07	-1854	-56.16	-3049
-2.379	-.2325	-3.300	-7.628	-10.56	-74.30	-13.71	-171.8	(6)		-31.29	-932.1	-48.26	-2162	-56.60	-3105
-2.396	-.3637	-3.401	-8.440	-10.73	-78.75	-13.94	-179.0	-26.52	-601.9	-31.96	-980.6	-50	-2304	-57.04	-3162
-2.418	-.5244	-3.511	-9.323	-10.89	-83.19	-14.18	-186.6	-26.88	-622.8	-32.32	-1006	(8)		-57.49	-3220
-2.439	-.7149	-3.631	-10.29	-11.05	-87.69	-14.43	-194.5	-27.18	-642.4	-32.68	-1032	-50.70	-2373	-58.43	-3339
-2.467	-.9355	-3.763	-11.35	-11.20	-92.29	-14.69	-202.3	-27.47	-661.6	-33.06	-1059	-51.20	-2429	-58.92	-3402
-2.498	-1.187	-3.910	-12.53	-11.35	-96.99	-14.97	-211.9	-27.75	-680.7	-33.45	-1088	-51.64	-2481	-59.42	-3466
-2.533	-1.468	-4.077	-13.88	-11.51	-101.8	-15.27	-221.6	-28.03	-699.9	-33.87	-1118	-52.06	-2532	-59.94	-3533
-2.572	-1.782	-4.271	-15.43	-11.67	-106.8	-15.60	-232.1	-28.30	-719.4	-34.31	-1149	-52.46	-2582	-60.48	-3602
-2.615	-2.127	-4.502	-17.30	-11.83	-111.8	-15.96	-243.8	-28.58	-739.0	-34.78	-1183	-52.86	-2632	-61.05	-3674
-2.662	-2.505	-4.792	-19.63	-11.99	-117.0	-16.38	-257.2	-28.86	-758.9	-35.29	-1220	-53.26	-2682	-61.65	-3751
Curve IV															
(4)		-8.586	-6.274	-9.518	-35.37	-20.74	-172.7	-22.85	-321.1	-26.02	-538.9	-42.67	-1318	-46.97	-1863
+∞	+∞	-8.624	-7.468	-9.612	-38.19	-20.88	-181.9	-23.21	-346.1	-26.39	-559.6	-42.94	-1351	-47.29	-1903
-2.746	180.2	-8.665	-8.768	-9.710	-41.14	-21.02	-191.2	-23.39	-359.0	-27.06	-589.7	-43.20	-1385	-47.61	-1944
(2)		-8.710	-10.17	-9.815	-44.21	-21.16	-200.7	-23.57	-372.2	-30.71	-713.7	-43.47	-1419	-47.95	-1986
-8.390	-.0518	-8.758	-11.68	-9.927	-47.44	-21.30	-210.5	-23.76	-385.6	-40	-1024	-43.74	-1454	-48.29	-2028
-8.394	-.2071	-8.809	-13.30	-10.05	-50.83	-21.44	-220.5	-23.95	-399.3	(6)		-44.02	-1488	-48.64	-2072
-8.403	-.4661	-8.863	-15.01	-10.19	-54.45	-21.58	-230.7	-24.15	-413.3	-40.56	-1064	-44.29	-1524	-49.01	-2116
-8.414	-.8286	-8.983	-18.78	-10.38	-58.46	-21.73	-241.2	-24.35	-427.5	-40.87	-1096	-44.58	-1560	-49.40	-2163
-8.429	-1.295	-9.048	-20.82	-10.69	-63.57	-21.88	-251.9	-24.56	-442.1	-41.14	-1127	-44.86	-1596	-49.84	-2213
-8.447	-1.865	-9.117	-22.97	-12.16	-77.65	-22.04	-262.8	-24.78	-456.9	-41.39	-1158	-45.44	-1670	-50.40	-2272
-8.468	-2.539	-9.189	-25.22	-20	-144	-22.19	-274.0	-25.00	-472.2	-41.65	-1189	-45.74	-1707	-51.44	-2365
-8.493	-3.316	-9.266	-27.59	(4)		-22.35	-285.4	-25.22	-487.8	-41.90	-1221	-46.04	-1745	-57.37	-2806
-8.521	-4.198	-9.346	-30.07	-20.42	-154.7	-22.52	-297.1	-25.46	-504.0	-42.16	-1253	-46.35	-1784	-68	-3600
-8.552	-5.184	-9.430	-32.66	-20.60	-163.7	-22.68	-309.0	-25.72	-520.8	-42.41	-1285	-46.65	-1823		
Curve VI															
(6)		-18.48	-5.565	-18.86	-32.84	-19.65	-89.26	(4)		-35.56	-405.4	-37.14	-606.3	-38.85	-822.4
+∞	+∞	-18.50	-7.269	-18.97	-41.04	-19.75	-95.78	-34.46	-273.3	-35.70	-423.7	-37.32	-628.7	-39.06	-848.6
-15.41	214.8	-18.53	-9.200	-19.03	-45.47	-19.85	-102.5	-34.61	-288.7	-35.85	-442.4	-37.49	-651.4	-39.27	-875.2
(2)		-18.56	-11.36	-19.10	-50.14	-19.95	-109.6	-34.75	-304.2	-36.00	-461.4	-37.68	-674.6	-39.49	-902.4
-18.40	-.1136	-18.59	-13.75	-19.17	-55.04	-20.06	-116.8	-34.88	-320.1	-36.15	-480.9	-37.86	-698.2	-39.73	-930.2
-18.40	-.4543	-18.63	-16.36	-19.24	-60.16	-20.19	-124.4	-35.01	-336.4	-36.31	-500.8	-38.05	-722.1	-39.98	-959.0
-18.41	-1.022	-18.67	-19.20	-19.32	-65.52	-20.34	-132.4	-35.14	-353.0	-36.47	-521.1	-38.25	-746.6	-40.28	-989.7
-18.42	-1.817	-18.71	-22.27	-19.40	-71.11	-20.65	-141.8	-35.28	-370.1	-36.63	-541.8	-38.44	-771.4	-40.96	-1033
-18.44	-2.839	-18.75	-25.57	-19.48	-76.93	-34	-256	-35.42	-387.6	-36.80	-562.9	-38.64	-796.7	-58	-1600
-18.45	-4.089	-18.80	-29.09	-19.56	-82.98										

TABLE 5.- SOLUTIONS OF FREQUENCY EQUATIONS (16) FOR $\alpha = \beta = \delta$ WITH VARIOUS VALUES OF RESTRAINT COEFFICIENT q_y (FIRST FOUR MODES)

q_y	δ for -			
	n = 1	n = 2	n = 3	n = 4
2	1.7855	3.2733	4.8063	6.3560
4	1.9068	3.3666	4.8808	6.4172
6	1.9833	3.4364	4.9412	6.4692
8	2.0374	3.4907	4.9910	6.5139
10	2.0778	3.5341	5.0328	6.5526
14	2.1344	3.5993	5.0989	6.6163
18	2.1723	3.6460	5.1488	6.6663
20	2.1868	3.6646	5.1694	6.6874
25	2.2152	3.7020	5.2116	6.7319
33.3	2.2464	3.7450	5.2621	6.7867
50	2.2815	3.7956	5.3240	6.8566
100	2.3207	3.8551	5.4006	6.9472
∞	2.3651	3.9271	5.5001	7.0652

2/22/85

"The aeronautical and space activities of the United States shall be conducted so as to contribute . . . to the expansion of human knowledge of phenomena in the atmosphere and space. The Administration shall provide for the widest practicable and appropriate dissemination of information concerning its activities and the results thereof."

—NATIONAL AERONAUTICS AND SPACE ACT OF 1958

NASA SCIENTIFIC AND TECHNICAL PUBLICATIONS

TECHNICAL REPORTS: Scientific and technical information considered important, complete, and a lasting contribution to existing knowledge.

TECHNICAL NOTES: Information less broad in scope but nevertheless of importance as a contribution to existing knowledge.

TECHNICAL MEMORANDUMS: Information receiving limited distribution because of preliminary data, security classification, or other reasons.

CONTRACTOR REPORTS: Technical information generated in connection with a NASA contract or grant and released under NASA auspices.

TECHNICAL TRANSLATIONS: Information published in a foreign language considered to merit NASA distribution in English.

TECHNICAL REPRINTS: Information derived from NASA activities and initially published in the form of journal articles.

SPECIAL PUBLICATIONS: Information derived from or of value to NASA activities but not necessarily reporting the results of individual NASA-programmed scientific efforts. Publications include conference proceedings, monographs, data compilations, handbooks, sourcebooks, and special bibliographies.

Details on the availability of these publications may be obtained from:

SCIENTIFIC AND TECHNICAL INFORMATION DIVISION

NATIONAL AERONAUTICS AND SPACE ADMINISTRATION

Washington, D.C. 20546